Chemical Engineering Journal 450 (2022) 138145

Contents lists available at ScienceDirect

Chemical Engineering Journal

journal homepage: www.elsevier.com/locate/cej

The journey of tuning chitosan properties in colloidal systems: Interactions with surfactants in the bulk and on the alumina surface

J. Matusiak [a,*], E. Grządka [b], U. Maciołek [c], E. Godek [b], E. Guzmán [d,e]

[a] Faculty of Chemistry, Wroclaw University of Science and Technology, Wybrzeże Wyspiańskiego 27, 50-370 Wroclaw, Poland
[b] Department of Physical Chemistry, Institute of Chemical Sciences, Faculty of Chemistry, Maria Curie-Sklodowska University in Lublin, M. Curie-Sklodowska Sq. 3, Lublin 20-031, Poland
[c] Analytical Laboratory, Institute of Chemical Sciences, Faculty of Chemistry, Maria Curie-Sklodowska University in Lublin, M. Curie-Sklodowska Sq. 3, Lublin 20-031, Poland
[d] Departamento de Química Física, Facultad de Ciencias Químicas, Universidad Complutense de Madrid, Ciudad Universitaria s/n, 28040 Madrid, Spain
[e] Unidad de Materia Condensada, Instituto Pluridisciplinar, Universidad Complutense de Madrid, Paseo Juan XXIII 1, 28040 Madrid, Spain

ARTICLE INFO

Keywords:
Stabilization
Flocculation
Alumina
Surface tension
Composites
Solid surface

ABSTRACT

The specific physico-chemical properties of chitosan (Ch), a biopolymer isolated from chitin, and its impact on the stability of colloidal dispersity have focused the interest of science and industry. However, in some cases chitosan alone is not enough to provide high stability to dispersions, making it necessary to add surfactant to the chitosan/oxide system, leading to superior stabilizing properties due to the association of polymer and surfactant molecules to form complexes that can modify the ability of bare chitosan for adsorbing on colloidal materials. This study explores the interactions between chitosan and alumina in the presence of three different anionic surfactants: the hydrocarbon SDS (sodium dodecyl sulfate), the fluorocarbon FS-91 (Capstone® FS-91), and the silicone A-Si (Silphos A-100). Different analytical methods evidenced chitosan adsorption on the alumina surface, forming hybrid organic–inorganic materials. This process can be enhanced by adding surfactant, with SDS leading to a strong increase of chitosan adsorption. Elemental mapping and scanning electron microscope imaging have provided a confirmation of the co-adsorption of polymer and surfactant on the alumina surface. The latter emerges as a very important finding because the results have shown that small quantities of surfactant (as low as 0.002% v/v) can strongly influence the adsorption and stability of multicomponent colloidal systems. This allows decreasing the chitosan amount required for the enhancement of the colloidal stability in relation to dispersions without added surfactants, providing the basis for reducing the production costs of colloidal dispersion, which opens new opportunities to chemical industry.

1. Introduction

In order for industry to fulfil the green challenge that demands eco-sustainable products and contribute to sustainable development, it needs to implement natural compounds, such as polysaccharides. This entails the replacement of synthetic and non-biodegradable compounds, many times derived from petroleum chemical sources, with biodegradable and biocompatible raw materials, preferably from renewable sources, e.g., chitosan [1,2].

Chitosan is a linear copolymer derived from the deacetylation of chitin, which is made by different molar fractions of D-glucosamine and *N*-acetyl glucosamine units distributed randomly along the polysaccharide chain [3]. This chemical structure allows the easy functionalization, which provides a broad range of applications of chitosan, including the manufacture of wound dressing, artificial skin, cosmetics, water engineering, paper finishing, metal chelating agents, design of drug delivery systems, tissue engineering, and fat trapper [4–9]. On the other side, the presence of a large number of amino and hydroxyl groups endows chitosan with a strongly adsorptive character while its cationic nature has offers benefits for the removal of anionic substances, e.g., dyes [10–12]. Also stabilizing [13] and flocculating properties [14] of chitosan can be used. However, the outcome of stabilization/flocculation depends on the environmental conditions, e.g., pH, ionic strength, presence of additives, etc. For instance, the addition of surface active agents can completely alter or change chitosan properties [15,16], allowing the increase or decrease of the colloidal stability

* Corresponding author.
E-mail address: jakub.matusiak@pwr.edu.pl (J. Matusiak).

https://doi.org/10.1016/j.cej.2022.138145
Received 26 May 2022; Received in revised form 4 July 2022; Accepted 14 July 2022
Available online 16 July 2022

of dispersions depending strongly on the mixture composition [17]. In fact, when the polymer and/or surfactant concentration is high, strong electrostatic interactions result in the formation of a macroscopic phase that alters system stability, which is caused by the removal of the factor (polymer or surfactant) governing system stabilization [18]. Once the macroscopic phase of the polymer-surfactant complexes is formed, the destabilization of the colloidal system may be brought about by the distribution of the complexes in the bulk. However, if the concentration of the polymer and/or surfactant is low, no macroscopic phase formation is expected [19]. In such a case, most likely no change in the stability of the system is observed. With the polymer concentration being enhanced (constant surfactant concentration), sandwich-like polymer-surfactant layers are formed. If the complexes adsorb on the solid surface, in most cases, an increase in stability is observed. On the contrary, if the complexes are characterized by a higher affinity toward the bulk phase, either stabilization or destabilization can occur [20–25].

The description of the stability in multicomponent colloidal systems is quite complicated, as many factors must be considered. Here, the stabilizing properties of chitosan over alumina suspensions in the presence of different anionic surfactants are investigated. Aluminium oxide is one of the most common colloidal materials used in the cosmetic and pharmaceutical industries [26]. Moreover, it is also one of the best characterized and most used adsorbents in different fields [27]. Therefore, its stabilization in liquid medium can impact decisively in the efficacy of different process and products. On the other side, the combination of low concentration of the surfactants with chitosan can be considered a very attractive concept for alumina stabilization that is not only scientifically relevant, but is also needed for the industry. In fact, the economic justification behind the use of relatively cheap surface-active agents, in small quantities, is undeniable. It is expected that the addition of oppositely charged surfactants in low concentration can provide an additional stability to the chitosan/alumina system. Despite its abundance, chitosan is harder to acquire than the commercially available surfactants. Moreover, from technological point of view it is easier to formulate products with soluble surfactants characterized by their low viscosity, than the use of polymers at higher concentrations. The novelty that we describe here is the use of different classes of surfactants, such as hydrocarbon, silicone, and fluorocarbon, for modifying chitosan properties. This is important because fluorocarbon and silicone surfactants are known to possess exceptional properties, sometimes superior to those of hydrocarbon ones [28,29]. We have decided to test the role of one surfactant from each family to obtain results that may be applied to a broad range of applications. SDS is one of the most popular surfactants with uncountable applications, that has been known to a mankind for ages [30]. On the other side, the fluorocarbon surfactant Capstone® FS-91 and the silicone surfactant are also interesting choices that may also contribute to different applications. Fluorocarbon surfactants are irreplaceable in the effective reduction of surface tension, while silicon surfactants due to their high surface activity and silicone character provide performance advantage and are used to create nanostructured materials. Since the concentration of the used surfactants was low (0.002 % v/v), and below their critical micelle concentrations (cmc), different effects associated with the addition of the surfactants may be expected: (i) no change in stability due to low or no interactions between chitosan and the surfactants used; (ii) increase in the stability due to the formation of sandwich-like adsorption layers composed by polymer-surfactant complexes adsorbed on the alumina surface, or (iii) decrease in stability related to the higher affinity of the formed complexes toward the bulk phase. To provide a framework describing the ongoing processes, different analytical methods have been exploited, allowing the characterization of the physicochemical properties of the systems and studying their adsorption and electrokinetic properties. Thus, it will be possible to determine whether surfactants can promote the stabilizing effect of chitosan for metal oxide suspensions. This is extremely important for different branches of industry, particularly the cosmetic one. For instance, chitosan is widely used in oral healthcare, haircare, and skincare products, and industrial formulators are constantly seeking new routes for improving the application of natural substances, many of them of colloidal nature. Therefore, the design of methodologies for the stabilization of such systems is crucial, and the use of chitosan as stabilizer and bioactive polymer can open new avenues for the cosmetic industry.

2. Materials and methods

2.1. Materials

Chitosan (medium molecular weight, product number 448877, batch number STBF3507V) was purchased from Sigma-Aldrich (Saint Louis, MO, USA) with deacetylation degree DD = 75 % (according to the manufacturer), and used without further purification. Chitosan average molecular weight (M_w) was determined by size exclusion chromatography (*SEC*) with a double detection system (refractive index, RI, and multi-angle light scattering, MALS). The value was 411 kDa, which corresponds to the value previously reported in the literature [13]. The content of carbon, nitrogen and hydrogen of chitosan was evaluated by means of elemental analysis (EuroEA3000 CHNS-O Analyser, EuroVector, Pavia, Italy); The values were 40.548 % w/w (C), 7.096 % w/w (N), and 8.439 % w/w (H).

Three anionic surfactants of different chemical nature were also used: a hydrocarbon surfactant, sodium dodecyl sulphate (SDS) from Sigma-Aldrich (Saint Louis, MO, USA); a fluorocarbon surfactant, Capstone® FS-91 from DuPont Corp. (Wilmington, DE, USA) containing CF_x groups in its hydrophobic tail and phosphate group (–O-PO-$(OH)_2$) as hydrophilic head, and a silicone surfactant – Silphos A-100 (A-Si) that can be classified as dimethicone PEG-8 phosphate, containing phosphate group as a hydrophilic part, from Siltech Corp. (East York, Canada).

Alumina (Al_2O_3) produced by Merck (Darmstadt, Germany) was used as an adsorbent. Since the adsorbent was of commercial origin, to avoid the influence of impurities on the results of experiments, before its use it was washed with doubly distilled water until the conductivity of the supernatant was lower than 2 μS cm^{-1}. X-ray diffraction (XRD) analysis confirmed that the used adsorbent is gamma-phase alumina. The analysis of the crystalline phases showed that the sample contained 97 % Al_2O_3 and 3 % hydrated Al_2O_3 (see Fig. S1 in Supporting Material). Figs. S2 and S3 (see Supporting Material) display the morphology of the adsorbent surface as was obtained from transmission electron microscopy (TEM, Titan G2) and scanning electron microscopy (SEM, Quanta 3D FEG). The sample preparation for TEM imaging is described in the Supplementary Material. The average size of the Al_2O_3 particles was estimated as the apparent diameter by light scattering using a Mastersizer 2000 (Malvern Instrument ltd., Malvern, UK), yielding a value of d = 13.10 μm, which overlaps with previously reported results [31].

3. Methods

3.1. Adsorption measurements

Chitosan aqueous solutions with concentrations in the range of 60–800 ppm with NaCl (0.01 mol/dm^3) as background electrolyte were prepared in 10 cm^3 flasks. Then, 0.2 g of Al_2O_3 was added to the 10 cm^3 solution. The resultant suspensions were shaken for 18 h in a thermostatic water bath at 25 °C (OLS 2000, Grant Instrument ltd., Shepreth, UK).

The determination of the concentration of free chitosan remaining in the solution after interaction with alumina was carried out with the modified ninhydrin method proposed by Prochazkova et al. [32]. For this purpose, 1 cm^3 of ninhydrin reagent was added to 1 cm^3 of the supernatant obtained from the centrifugation of the dispersion containing chitosan and alumina at a speed of 14000 rpm in a high-speed centrifuge (310b, Precision Engineering, Andover, UK). The solutions were heated in a laboratory oven (UNE 400, Memmert GmbH,

Schwabach, Germany) at 100 °C for 30 min. Afterwards, the samples were equilibrated to room temperature, and then 5 cm^3 of 50 % v/v ethanol solution was added to each of them and mixed in a laboratory vortex for 15 s. Finally, the absorbance of the final mixtures was measured at 570 nm with a UV–Vis spectrophotometer (Cary 100, Varian Instruments, Palo Alto, CA, USA). All measurements were repeated four times and the resultant values were averaged.

In the case of the adsorption of the chitosan/surfactant complexes the same analytical methodology was applied. First, 10 cm^3 of solutions containing: NaCl (0.01 mol/dm^3), chitosan (60–800 ppm), surfactant (0.002 % v/v) and bi-distilled water were prepared. Then, 0.2 g of alumina was added to the solution. The suspensions were shaken for 18 h in a thermostatic water bath at 25 °C.

3.2. Evaluation of the chitosan-surfactants interactions

The optical tensiometer Theta (KSV Instruments ltd., Espoo, Finland) determined the surface tension (pendant drop method). Surfactant solutions were prepared by adding surfactant stock solutions (SDS, FS-91, A-Si) to the flasks up to a total volume of 50 cm^3 to obtain solutions with concentrations in the desired ranges (SDS: 0–0.3 % v/v, FS-91: 0–0.6 % v/v, A-Si: 0–0.6 % v/v). For the set of measurements performed in the presence of chitosan, the appropriate volume of the polymer stock solution (1000 ppm in 0.1 mol/dm^3 acetic acid) was added to the flasks containing the surfactant, so chitosan concentration was fixed in 400 ppm. The measurements were carried out at room temperature (25℃). The values from five independent measurements were averaged.

The same solutions containing chitosan and the surfactants (SDS, FS-91, A-Si) were analyzed by electrophoretic mobility using a Zetasizer Nano ZS (Malvern Instruments ltd., Malvern, UK). The electrophoretic mobility was measured and recalculated to the zeta potential with the Smoluchowski approach. The resultant zeta potential for the pure chitosan solution (400 ppm) was 57.2 mV. The values from five independent measurements were averaged.

3.3. Stability measurements

The effect of Ch and Ch/surfactant complexes on the stability of the alumina suspensions was investigated adopting a spectrophotometric method. The suspensions with a volume of 10 cm^3 containing 0.005 g of alumina, background electrolyte (0.01 mol/dm^3 NaCl) and the bi-distilled water were prepared and sonicated for 30 s (750 W, 20 kHz, Sonics Vibra Cell, Sonics & Materials Inc., Newton, CT, USA). Afterwards, the fixed volume of Ch stock solution was added to the samples to obtain mixtures with a final chitosan concentration of 400 ppm. In the case of systems also containing surfactants, the calculated volume of these compounds was added up to a final concentration of 0.002 % v/v. The obtained suspensions were scanned for 15 h (Cary 300, Varian Instruments, Palo Alto, CA, USA) with bi-distilled water as a reference. The whole spectra in the range 200–800 nm were collected, and the single wavelength was chosen. Data were evaluated as the time evolution of the absorbance (at $\lambda = 500$ nm).

3.4. Zeta potential measurements

0.01 g of alumina were added to the 100 cm^3 solution of the background electrolyte NaCl (0.01 mol dm^{-3}). The suspensions were ultrasonificated for 3 min (Sonics Vibra Cell, Sonics & Materials Inc., Newton, CT, USA). Afterwards, Ch was added to the colloidal suspension to reach the polymer concentration (100 ppm). In the case of systems containing surfactants, the calculated volumes of these compounds were added to the mixture to a concentration of 0.002 % v/v. The pH of the suspensions was adjusted by adding HCl and NaOH solutions (pH = 3–10). The electrophoretic mobility was measured with Zetasizer Nano ZS (Malvern Instruments, ltd., Malvern, UK) and converted to the zeta potential by the Smoluchowski approach. All measurements were made four times and the values were averaged.

3.5. Characterization of the Ch and Ch/surfactant complexes adsorption on alumina

A detailed characterization of the effect of Ch and Ch/surfactant complexes on the alumina properties was obtained before and after the adsorption process of the systems containing chitosan. For this purpose, pre- and post-adsorption alumina samples were dried in a laboratory oven at 80 °C until no significant change in mass was observed and used for further studies.

A Fourier-transform infrared spectrometer Nicolet 8700 FTIR (Thermo Fisher Scientific, Waltham, MA, USA) was used to collect the spectra in the transmission mode within the mid-infrared range (4000–400 cm^{-1}) at a resolution of 4 cm^{-1} with the application of the KBr pressed disc method (4 mg of sample per 200 mg of KBr). The spectrometer was equipped with the DLaTGS (KBr window) detector, EverGlo mid-IR source, and mid-IR optimized Ge-on-KBr beamsplitter. Sixty-four scans were averaged for each spectrum.

The specific surface area (SSA), micropore area and volume of the samples were obtained through the low-temperature adsorption–desorption of nitrogen at 77 K in Accelerated Surface Area and Porosimetry System (ASAP 2420, Micromeritics Corp., Norcross, GA, USA). The standard Brunauer-Emmett-Teller (BET) method was employed to calculate the SSA, whereas *t*-Plot analysis was applied to calculate the micropore area and volume. Prior to measurements, the samples were degassed at 120 °C.

A Scanning Electron Microscope (SEM) Quanta 3D FEG (FEI Co., Hillsboro, NE, USA) was used to analyse the changes in the morphology of the samples before and after adsorption. To study the aggregation of the particles after adsorption, an Everhart-Thornley detector (ETD) with a voltage of 5 kV and a magnification of 100x was used. High resolution micrographs obtained by a backscattering electron detector BSED (20 kV, magnification 1000x) provided information about the morphology of the alumina surface after the adsorption of chitosan-surfactant complexes. The elemental mapping of the studied samples was carried out by means of the BSED detector (magnification 1000x) by Energy Dispersive Spectroscopy (EDS) using an Octane Elect Plus system (EDAX, Pleasanton, CA, USA).

The changes on the surface chemistry of the samples after adsorption was evaluated by X-ray photoelectron spectroscopy (XPS) with an ultra-high vacuum multichamber analytical system (Prevac, Rogów, Poland). To collect the XPS spectra, the Scienta R4000 electron analyzer was employed. Monochromatic X-ray Al Kα source (Scienta SAX-100 X-ray source) was used during the experiments. All binding energies were calibrated with respect to the characteristic of aromatic carbon C1s band at 284.7 eV.

4. Results and discussion

4.1. Formation of chitosan-surfactant complexes in solution

A very important aim of this study is to evaluate whether the formation of complexes between chitosan and three different anionic surfactants can alter the ability of chitosan for modifying the properties and stability of alumina colloids. To this end, it is interesting to analyse the formation of chitosan/surfactant in solution before exploring its interaction with alumina. The evaluation of the change of the polymer zeta potential with the addition of a surfactant provides important insights into the surfactant binding to the polymer chains. Fig. 1a-c show the evolution of the zeta potential of chitosan with the addition of incremental concentrations of the anionic surfactants.

The addition of anionic surfactants should lead to the neutralization of the charge of the chitosan chain due to electrostatic binding. Considering that the zeta potential of pure chitosan solution (400 ppm) was estimated to be 57.5 mV, progressive reduction in these values

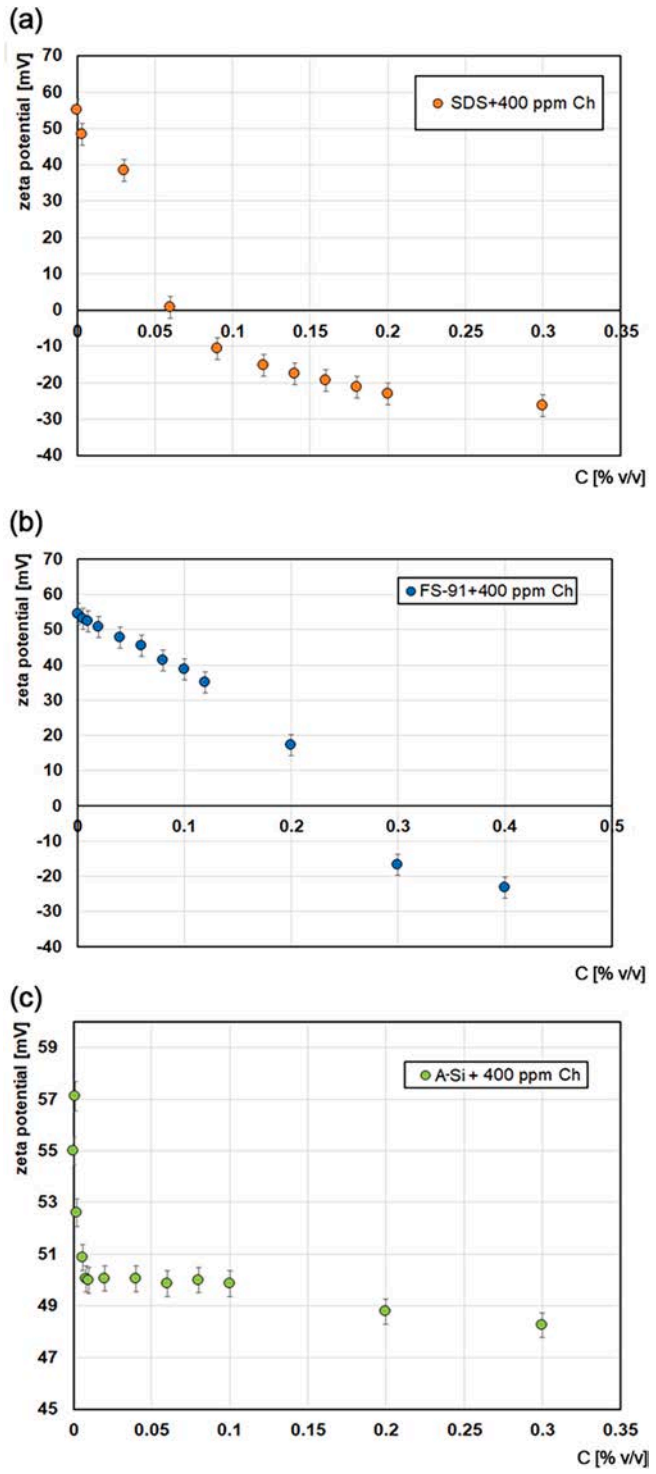

Fig. 1. Changes of the zeta potential of chitosan (Ch) in the presence of (a) SDS, (b) FS-91 and (c) A-Si.

might be expected as anionic surfactants are added. The results evidence that this is not the picture emerging from the mixtures of chitosan with the three surfactants. In the case of the Ch/SDS system, the surfactant binding leads to a progressive neutralization of the chitosan charge till it reaches the neutralization point for the SDS concentration of about 0.05 % v/v. A further increase in the added concentration of SDS leads to the formation of negatively charged complexes. A similar evolution of the zeta potential with the addition of surfactant was found for the Ch/FS-91 system. The inversion of the complex charge for this system is shifted to a surfactant concentration more than 5 times higher than in the Ch/SDS systems (well above 0.2 % v/v). It should be noted that the phenomenon found in the mixtures of chitosan with SDS and FS-91 is the most common in the formation of polyelectrolyte/surfactant systems [33]. On the other side, the effectivity of the electrostatic binding of A-Si to chitosan is very limited, and the Ch/A-Si complexes are characterized by positive values of the zeta potential in the whole range of studied concentrations.

Further details on the association of chitosan and the three anionic surfactants can be obtained from surface tension measurements. Fig. 2a-c show the surface tension dependences for the adsorption at the water/vapour interface of the three anionic surfactants and their mixtures with chitosan.

The values of the critical micelle concentrations (cmc) for the surfactants agree with values correspond to those reported in the literature [34]. The analysis of the surface tension curves points to additional conclusions as to the polymer/surfactant interactions [35]. These appear strongly dependent on the specific nature of the surfactant in agreement with the differences on the electrostatic binding inferred from the zeta potential results. The formation of the Ch/SDS complexes leads to a synergistic effect in the reduction of the surface tension in relation to pure SDS. Thus, even though the dependences of the surface tension of both SDS and Ch/SDS solutions on the surfactant concentration are similar, characterized by the monotonous decrease in the surface tension to reach the cmc, the surface tension values for Ch/SDS always appear below those of SDS for the same solution, which correspond to what is found for most polycation/anion surfactant systems [36]. This is analogous to the strong affinity of SDS for the chitosan chains, which favours the formation of polyelectrolyte/surfactant complexes. If the surface tension curves corresponding to the systems with the other two surfactants are considered, the outcome is different. In the case of the Ch/A-Si system, the interaction between the surfactant and the chitosan results in a worsening of the ability of the surfactant to reduce the surface tension of the water/vapor interface. This can be understood if we consider that even though the binding of the chitosan to A-Si is rather limited as evidenced by the zeta potential values, there is a certain degree of binding which may result in a mixture of non-surface active Ch/A-Si complexes and a non-negligible amount of free surfactant molecules This leads to a decrease in surface tension by the free surfactant molecules. Hence the values of the surface tension in the Ch/surfactant system are higher than those corresponding to the pure surfactant solution of the same concentration. This results from the depletion of a certain surfactant molecules from the solution upon their interactions with the chitosan. It should be noted that the differences between A-Si and the Ch/A-Si solutions are minimized with the increase in surfactant concentrations, which corresponds to the very limited binding of this surfactant in agreement with the zeta potential results. The case of FS-91 is even more complex. The dependences of the surface tension on surface concentrations appear similar for both surfactant and polymer/surfactant mixtures, even though there is evidence of the Ch/surfactant binding from the zeta potential measurements. It may be assumed that the surface activities of FS-91 and Ch/FS-91 are rather similar. Similar behaviour has been reported in the literature for the interaction of polycations and zwitterionic surfactants [37].

4.2. Adsorption of chitosan and the chitosan-surfactant complexes on the alumina surfaces

The modification of alumina as a result of the adsorption of chitosan and surfactants was initially assessed by the modification of the FTIR spectroscopy. The FTIR spectra of chitosan, Al_2O_3, and the Ch/Al_2O_3 mixtures are shown in Fig. 3a, while the corresponding spectra of the different Ch/surfactant/Al_2O_3 mixtures compared to those of chitosan and Al_2O_3 are displayed in Fig. 3b-d.

A broad band in the 3442–3425 cm^{-1} region of chitosan spectrum corresponds to the stretching vibration of the N—H and O—H groups forming hydrogen bonds. The absorption bands at 2921 and 2878 cm^{-1}

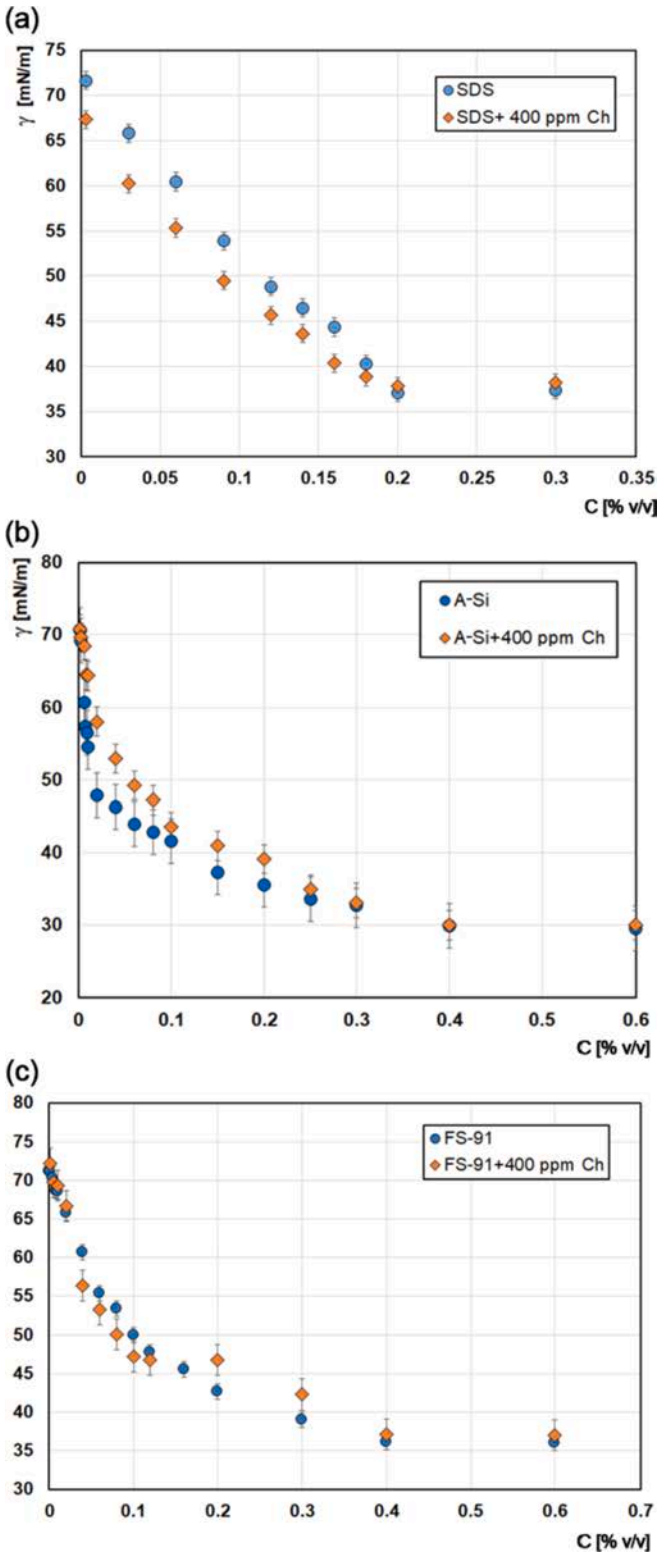

Fig. 2. Surface tension dependences on the surfactant concentration for the adsorption at the water/vapour interface of the three anionic surfactant and their mixtures with chitosan (Ch): (a) SDS, (b) A-Si and (c) FS-91.

can be assigned to symmetric and asymmetric C—H stretching, respectively. The presence of residual *N*-acetyl groups was confirmed by the bands at around 1655 cm^{-1} (C═O stretching of Amide I overlapping the N—H bending of Amide II) and 1322 cm^{-1} (C—N stretching of Amide III), respectively. A wide shoulder centred at 1589 cm^{-1} corresponds to the NH_2 bending (Amide II) of the primary amines [38]. The bands at 1422 and 1382 cm^{-1} originate from symmetrical deformations of CH_2 and CH_3 groups. These wavenumbers are also characteristic of O—H bending mode of monosaccharide units. The signal at 1154 cm^{-1} can be attributed to asymmetric stretching of the C—O—C polysaccharide bridge, while the strong bands at 1154 and 1033 cm^{-1} correspond to C—O skeletal stretching vibrations. The weak signal at 895 cm^{-1} is attributed to the C—H out of the plane vibration of the ring of monosaccharides, while the very wide band centred at around 614 cm^{-1} is characteristic for N—H and O—H bending out of the plane modes. The assignments of the absorption bands are consistent with the chitosan spectra reported in the literature [39–43].

In the FTIR spectrum of Al_2O_3, the adsorption bands at around 3464 and 1637 cm^{-1} are attributed to the stretching and bending vibration of the various structural O—H groups and adsorbed water, respectively. Two broad bands between 1100 and 400 cm^{-1} confirm the existence of alumina in the γ-form [44]. The band centred at 916 cm^{-1} is characteristic of Al−O vibrations in the O−Al−O and Al−O−Al bridges, while the Al−O stretching vibration was observed at 522 cm^{-1} [42,43,45,46]. The interaction of alumina and chitosan results in a FTIR spectrum for the Al_2O_3/Ch composite which presents several modifications with respect to the individual component. Firstly, the composite presents all the bands corresponding to chitosan groups, but their intensities are significantly reduced in relation to the bare chitosan which may indicate the adsorption of the biopolymer on the alumina. It was also observed that the band characteristics corresponding to Al_2O_3 dominate in the FTIR spectrum of the Al_2O_3/Ch composite (Fig. 3a). The red shift of the N—H bending band (from 1652 cm^{-1} in pure chitosan to 1630 cm^{-1} in the composite) as well as the blue one of the O—H and the N—H stretching bands (from 3442 cm^{-1} in pure chitosan to 3474 cm^{-1} in the composite) indicate the possible interactions between these functional groups and the Al_2O_3 particles. This may be understood considering the variety of OH groups on the alumina surface which makes possible the formation of hydrogen bonds with the OH and NH groups of the chitosan [47]. The reduced intensity of C—O stretching vibrations between 1154 and 1033 cm^{-1} further confirmed the binding of chitosan onto Al_2O_3. A decrease in the intensity of the band of Amide I (1652 cm^{-1}) accompanied by a reduction in the intensity of the band at 1382 cm^{-1} (CH_3 deformation) indicates a partial hydrolysis of the *N*-acetyl D-glucosamine units. These findings indicate that functional groups such as $–NH_2$, –OH, and –CO- are involved in the formation of the Al_2O_3/Ch composite.

Anionic surfactant-modified alumina has been widely studied because the high surface area and a positive charge at the solution pH below its point of zero charge offers a good platform where anionic surfactants such as SDS, A-100, and FS-91 can adsorb [48–50]. The FTIR spectra of Ch/surfactant/Al_2O_3 mixtures are presented in Fig. 3(b-d) together with the spectra of pure chitosan and bare alumina. The spectral analysis shows that the addition of surfactants has a slight effect on the adsorption of chitosan, regardless of the type of surfactant used. The band profiles of the FTIR spectra of the three ternary mixtures and the Ch/Al_2O_3 composite are complementary. Similarly to the Al_2O_3/Ch composite, a comparable reduction in the intensity of the N—H bending vibration at 1654 cm^{-1} and the bands in the regions of 1500–1300 and 1200–1000 cm^{-1}, characteristic of chitosan, is observed for the three ternary mixtures. This may be rationalized considering that the low concentration of the used surfactants (0.002 % v/v) is not enough to be detected by FTIR spectroscopy. A more quantitative evaluation of the effect of the additives on the FTIR spectrum of alumina can be performed by comparing the FTIR spectra of chitosan mixtures prepared without and with the addition of the anionic surfactants (see Fig. S4). It is possible to evaluate the influence of the anionic surfactants on the Ch/Al_2O_3 spectrum. The addition of surfactants modifies the Ch/Al_2O_3 spectrum in the wavelength region between 1200 and 400 cm^{-1}.

The absorbance peaks at 1654 and 1598 cm^{-1} (N—H bending) and 3474 cm^{-1} (O—H stretching overlapping the N—H stretching of the

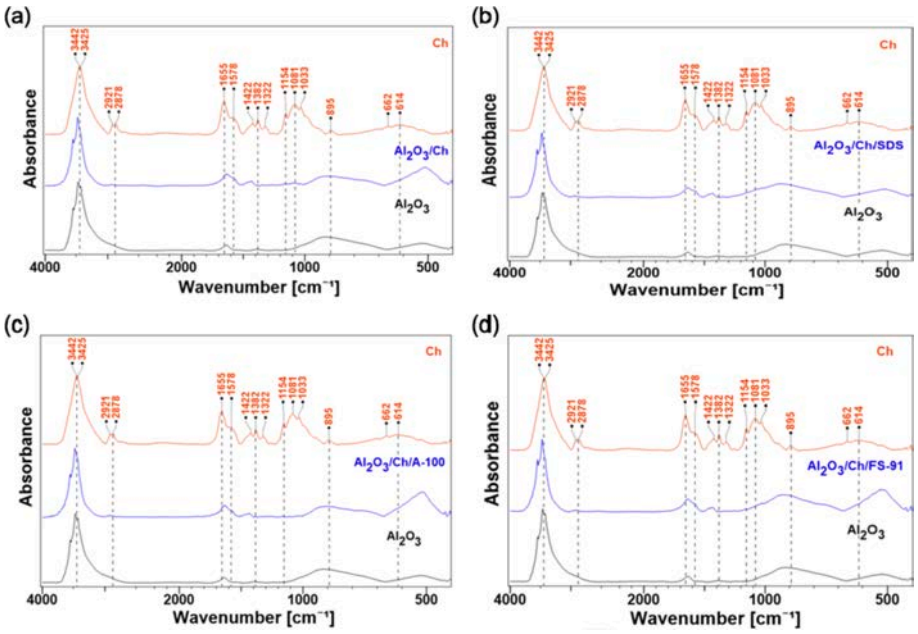

Fig. 3. FTIR spectra of chitosan, Al_2O_3 and Al_2O_3/Ch (a), Al_2O_3/Ch/SDS (b), Al_2O_3/Ch/A-100 (c) and Al_2O_3/Ch/FS-91(d) mixtures.

primary and secondary amine) indicate the presence of chitosan in the composites, while the two broad bands between 1200 and 400 cm^{-1} may be associated with the addition of surfactants.

The presence of chitosan and the Ch/surfactant complexes influences the physicochemical and structural properties of the aluminium(III) oxide. Table 1 represents the changes in the specific surface area (SSA), micropore area (MA) and micropore volume (MV) upon the adsorption of Ch and the Ch/surfactant mixtures on alumina surface. It can be observed that the SSA decreases after the adsorption of the polymer, whereas the Ch/surfactant complex adsorption does not lead to any further modification of SSA. There are no significant differences between the effects of the different surfactants on the SSA of the alumina. The reduction in the SSA upon the adsorption of chitosan and Ch/surfactant complexes can be understood in the light of the formation of a polymer or polymer/surfactant layer on the alumina, which results in the clogging of the alumina pores, reducing the available area of the alumina surface. This is confirmed by the impossibility to measure the MA and MV of the alumina samples after adsorption of the polymer or the polymer/surfactant complexes. In this case, a certain aggregation of the alumina colloids mediated by the formation of a chitosan or chitosan/surfactant layers cannot be ruled out on the basis of the changes of SSA.

The modification of the structure of the alumina surface as result of the adsorption of Ch and Ch/surfactant complexes inferred from the change of the SSA can be confirmed by the SEM micrographs reported in Fig. 4a-e.

The SEM micrographs show a significant aggregation of the solid alumina particles as a result of the adsorption of the polymer and its mixtures with the three surfactants. The samples are highly aggregated after the formation of the polymer or the polymer/surfactant layers. This may be due to the fact that the chitosan acts as glue by forcing the aggregation of the solid particles. In the case of the Ch/FS-91/Al_2O_3 and that of Ch/A-Si/Al_2O_3 systems, the polymer-surfactant complexes adsorb as a root (Fig. 5a) or loose spider-net (Fig. 5b), covering the alumina particles, respectively. In the case of Ch/SDS/Al_2O_3 system, the formed complexes are adsorbed on the alumina surface (Fig. 5c). The results suggest that in the Ch/SDS/Al_2O_3 system the organic polymer/surfactant complexes are directly bound to the alumina surface, whereas in the case of the Ch/FS-91/Al_2O_3 and Ch/A-Si/Al_2O_3 systems, the organic complexes are loosely deposited on the alumina, which was evidenced during the analysis (the organic layers were mobile under the electron beam).

SEM-EDX elemental mapping was carried out to reveal further details of the mechanism underlying the formation of chitosan and the Ch/surfactant layers (Fig. 6a-d). This might confirm that the applied surfactants control the morphology of the adsorption layer formed by the polymer-surfactant complexes.

The maps obtained from the elemental analysis Fig. 6a-d present the overlapped content of the different elements evidenced by different colours. In the case of the Ch/Al_2O_3 composite (Fig. 6a), the deposited chitosan forms flakes which are composed, as expected, mainly of carbon and nitrogen. The presence of these elements together with aluminium and oxygen confirms the deposition of the chitosan layer because carbon and nitrogen are not present in alumina, which is quite similar to the Ch/SDS/Al_2O_3 mixture. In this case, the elemental analysis also shows the presence of sulphur, which confirms the deposition of polymer-surfactant complexes on the alumina surface (Fig. 6b). However, when the Ch/A-Si/Al_2O_3 system is considered, the elemental analysis evidenced that the formed complexes do not present a significant adhesion to the alumina surface (Fig. 6c). Something similar was found for the Ch/FS-91/Al_2O_3 system. The 'spider-web' complexes that were present on the surface of alumina were composed of carbon, nitrogen, oxygen, and fluorine (Fig. 6d). Since the adsorption of the Ch/A-Si and Ch/FS-91 on alumina is very reduced, it can be assumed that the formed complexes are characterized by higher affinity for the bulk phase than for the alumina surface. However, a very small fraction of them can be still adsorbed on the solid surface, which occurs in this case as a loose organic fraction hooked to the alumina surface. This agrees with the above discussed surface tension results.

Table 1
SSA, MA and MV values of Al_2O_3 before and after the adsorption of Ch and Ch/surfactant mixtures.

	SSA [m^2/g]	MA [m^2/g]	MV [cm^3/g]
Al_2O_3	108.19 ± 0.17	3.67	0.000613
Al_2O_3/Ch	99.32 ± 0.58	–	–
Al_2O_3/Ch/SDS	98.38 ± 0.60	–	–
Al_2O_3/Ch/FS-91	98.33 ± 0.58	–	–
Al_2O_3/Ch/A-Si	97.74 ± 0.57	–	–

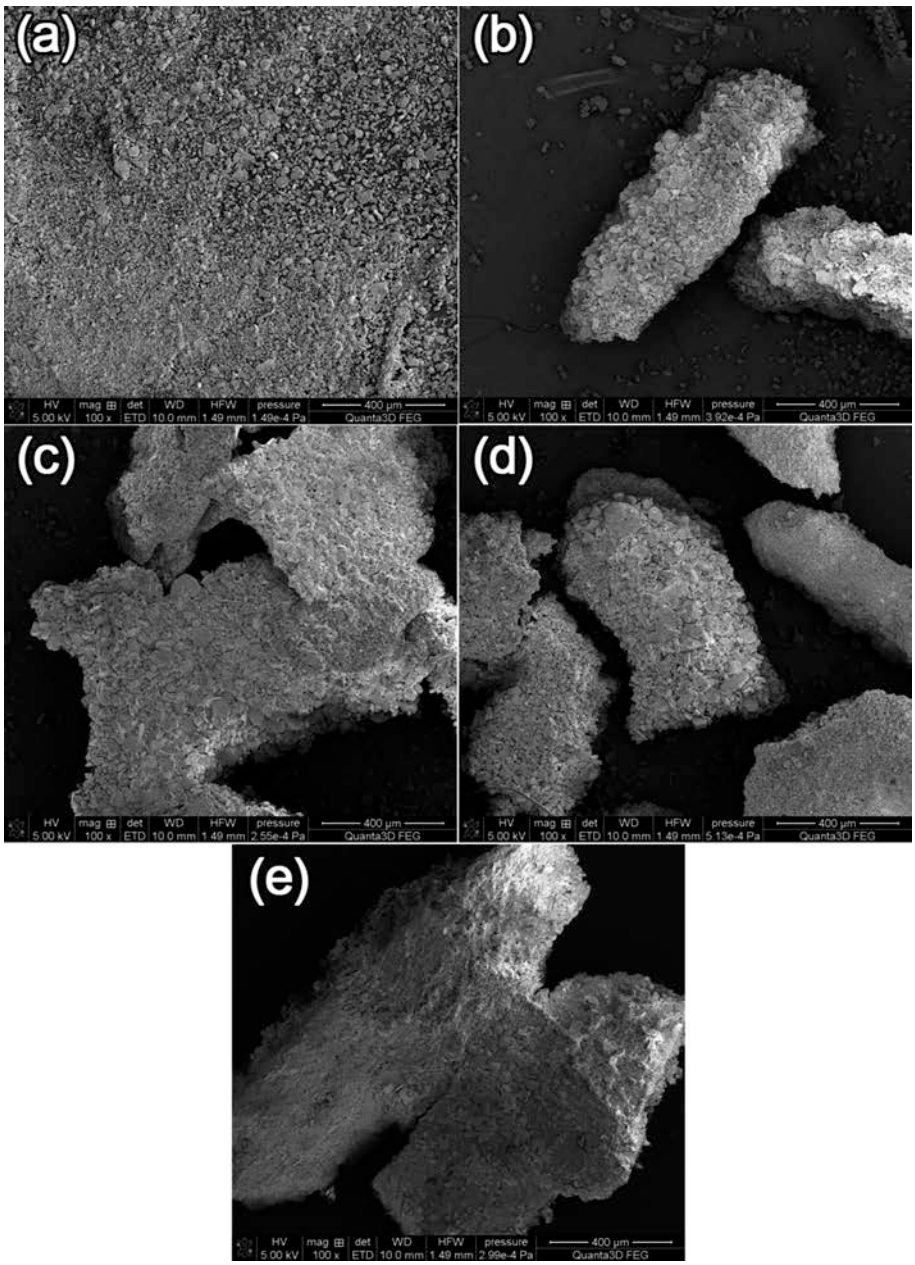

Fig. 4. SEM micrographs obtained for: (a) Al_2O_3, (b) Ch/Al_2O_3 composite, (c) Ch/SDS/Al_2O_3 mixture, (d) Ch/A-Si/Al_2O_3 mixture, (e) Ch/FS-91/Al_2O_3 mixture. All the images were obtained at 100x magnification.

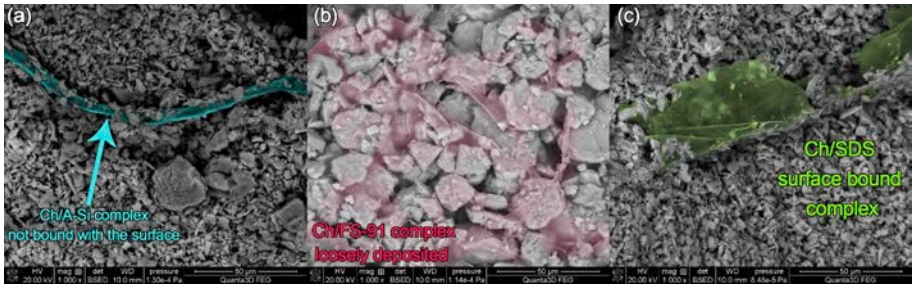

Fig. 5. Micrographs of the three ternary mixtures obtained a 1000x magnification: (a) Ch/A-Si/Al_2O_3, (b) Ch/FS-91/Al_2O_3, (c) Ch/SDS/Al_2O_3.

The nature of the surfactant plays a very important role in the control of the chitosan deposition. Further evidence on this issue can be extracted from the analysis of the amount of chitosan adsorbed on the alumina. Fig. 7 demonstrates the influence of anionic surfactants (SDS, A-Si and FS-91) on the amount of deposited chitosan on the alumina surface.

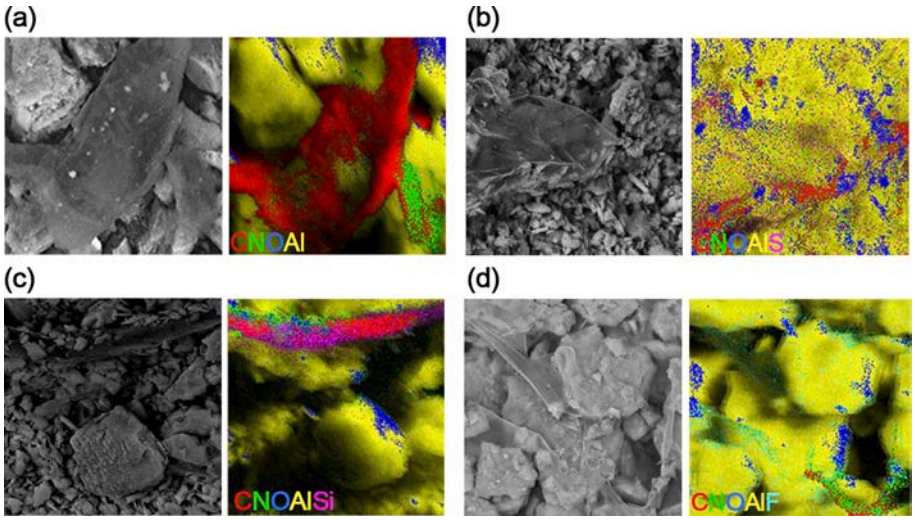

Fig. 6. SEM micrographs (left) and elemental analysis maps (SEM-EDX, right) for the different mixtures: (a) Ch/Al_2O_3, (b) Ch/SDS/Al_2O_3, (c) Ch/A-Si/Al_2O_3, (d) Ch/FS-91/Al_2O_3. The presence of different elements is evidenced by different colours.

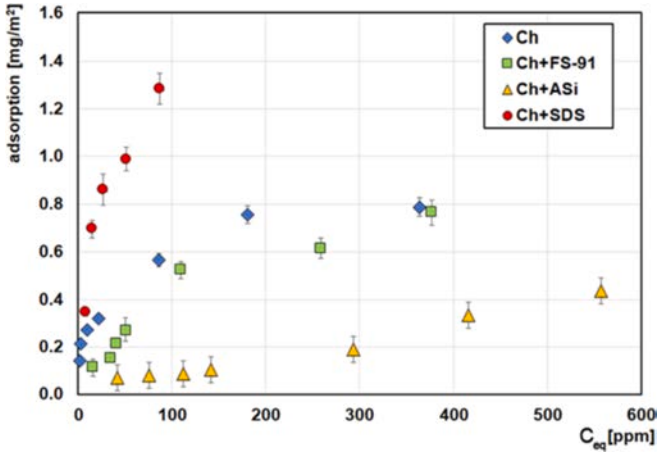

Fig. 7. Influence of the different surfactants (0.002% v/v) on the amount of deposited chitosan on the alumina surface as a function of the dependence of the adsorbed amount on the equilibrium concentration of chitosan on the initial solution (C_{eq}). For the sake of comparison, the results corresponding to the adsorption of chitosan in absence of surfactant are also plotted.

The results show that the adsorption of Ch on alumina increases from the smallest values of the equilibrium concentration of the chitosan in the solution (C_{eq}) up to reach a maximum adsorption of about 0.8 mg/m^2 for C_{eq} of about 200 ppm. This adsorption can be rationalized considering that chitosan has a hydrophilic nature due to the presence of hydroxyl groups (–OH) at the C-3 and C-6 positions and amino groups (–NH_2) at the C-2 position (pKa ≈ 6.3–7), which facilitates its interaction with the oxide surface by different mechanisms depending on the pH value [51,52]. At acidic pH (<6.5), chitosan is positively charged but at higher pH it loses its charge and may precipitate from solution due to the deprotonation of the amino groups [53]. It has already been proven that above the pKa values, chitosan tends to form nanoparticles, whereas it becomes completely insoluble at pH≈9.8 [54]. It was also observed that with an approximately equal ratio of *N*-acetyl glucosamine to D-glucosamine units chitosan will not precipitate from the system even above the pKa [55]. Taking into account that the adsorption of Ch on the alumina surface was conducted at pH≈7, when the surface of alumina is slightly positively charged (Notice that the pH of the isoelectric point of the alumina, pH_{iep}, is found around 6.5), whereas chitosan amine groups are not fully protonated, the most probable adsorption mechanisms of Ch on the alumina surface are hydrogen bonding and van der Waals interactions [56,57]. Due to the presence of Coulomb repulsion forces between substances of the same charge the electrostatic interaction is much less probable. In such cases the amine groups present in the chitosan chains are only partially protonated, which is why the polymer chain adopts a coiled conformation [58].

The addition of anionic FS-91 and A-Si surfactants to the Ch/Al_2O_3 leads to the formation of the polymer-surfactant complexes worsening the chitosan adsorption, which agrees with the elemental mapping results. This is due to the formation of the Ch/surfactant complexes having lower affinity to the alumina surface than chitosan. This can be understood considering that under the adsorption conditions, i.e., pH = 7 and a surfactant concentration of 0.002 % v/v, the Ch/FS-91 and Ch/A-Si complexes are positively charged. Therefore, if the adsorption of such complexes occurs on the alumina surface (predominantly in the Ch/SDS system), the process should be guided by non-electrostatic interactions. The possibilities of non-electrostatic interactions are diminished upon the binding of the surfactant to the chitosan chains due to the decrease in the number of available groups which reduces the interactions opportunities between the complexes and the alumina. On the other hand, the affinity of the complexes for the aqueous medium also plays a very important role on their limited adsorption in water. The formation of the Ch/A-Si complexes is associated with an enhanced solubility in relation to the surfactant. It may be expected that the formed complexes do not present any tendency to be depleted from the solution to the alumina surface, and when they absorb, they form a fuzzy layer protruding to the bulk. The results suggest that the adsorption of individual surfactant molecules on the alumina through electrostatic interactions cannot be ruled out. In the case of the Ch/FS-91 complexes, their solubility is very similar to that of the surfactant as evidenced by their similar surface activity, which can result in a reduced adsorption of the complexes on the alumina surface.

The worsening of the chitosan adsorption in the presence of FS-91 is lower than that of A-Si. This can be put down to the fact that the complexes of Ch and A-Si are characterized by a very reduced binding, having positive charge throughout the whole studied concentration range (as evidenced by the zeta potential values), which limit the complex depletion from the solution to the alumina surface. The binding in the Ch/FS-91 complexes is higher, and this can favour a certain depletion of the complexes to the surface; even the deposited amount remains below that corresponding to bare chitosan. Further details on the interactions between the polyelectrolyte/surfactant systems can be inferred from the zeta potential values of the suspensions depicted in

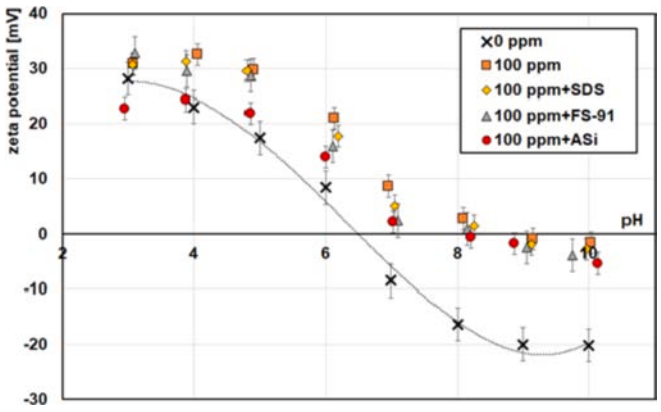

Fig. 8. Zeta potential of the alumina suspensions with different additives as function of the pH. Chitosan concentration 100 ppm and surfactant concentrations (0.002 % v/v).

Fig. 8.

The alumina suspension without any additives is positively charged up to pH = 6.5 (pH_{iep}). Above this pH value it starts to be negatively charged. This situation changes after the addition of chitosan. This cationic polysaccharide is rich in positively charged groups, forming a layer on the alumina surface, with positive residues protruding to the aqueous phase, which leads to the increase of the zeta potential in the entire measured pH range. The zeta potential increase is not proportional to the concentration of the protonated amino groups present in the system, since even a small number of positively charged $–NH_3^+$ could lead to the increase in the zeta potential. This also shows that above pKa of chitosan (greater than6.5), up to pH = 9, the zeta potential of the Ch/Al_2O_3 is still slightly positive. This indicates the role of the chitosan amine groups in the charge formation of the alumina dispersion, even above the pKa value of chitosan.

The addition of the anionic surfactants to the Ch/Al_2O_3 system slightly decreases the zeta potential. It is a result of the neutralisation reaction between cationic Ch and anionic surfactants. As one can see in the Ch/Al_2O_3 and Ch/Al_2O_3/surfactant systems the zeta potential is positive up to pH = 8 and even under pH values higher than 8 the zeta potential of the studied system is close to zero or only slightly negative. The lowest zeta potential values among the Ch/surfactant/Al_2O_3 systems are for A-Si, which could indicate the more expanded structure of the adsorption layer. This might also explain why the adsorption of the Ch/A-Si complexes is the lowest: looser complexes adsorbing on the alumina surface block free adsorption centres because of the steric reasons. On the other hand, the increase of the Ch adsorption on Al_2O_3 in the presence of SDS is also a consequence of the Ch/surfactant complexes formation. In this case the formed complexes are easily adsorbed on the solid surface, which reveals the strong binding of the anionic surfactant to the chitosan. There is also a possibility that the formed Ch/SDS complexes can contain more than one polymer macromolecule [59,60]; thus, if the number of the adsorption centres on the alumina surface is constant, the adsorption of such aggregates causes the increase in the total adsorption [61].

The adsorption data were confirmed by X-ray photoelectron spectroscopy (XPS). [43 44]. The XPS spectra (Fig. 9) confirm the adsorption of chitosan on the alumina surface. On the post-adsorption sample, peaks indicative of the presence of nitrogen and alumina were found (N 1 s, Al 2 s and Al 2p). In the case of chitosan, the presence of calcium was also noticed. Since the polymer is of natural origin, the presence of inorganic cations such as calcium, magnesium, sodium and potassium can be expected [62]. As far as the spectra of the hybrid materials containing surfactants are concerned, there were no significant changes opposed to Ch/Al_2O_3 samples (Fig. S5). The absence of sulphur, silicon and fluorine can be explained by too low a concentration of the

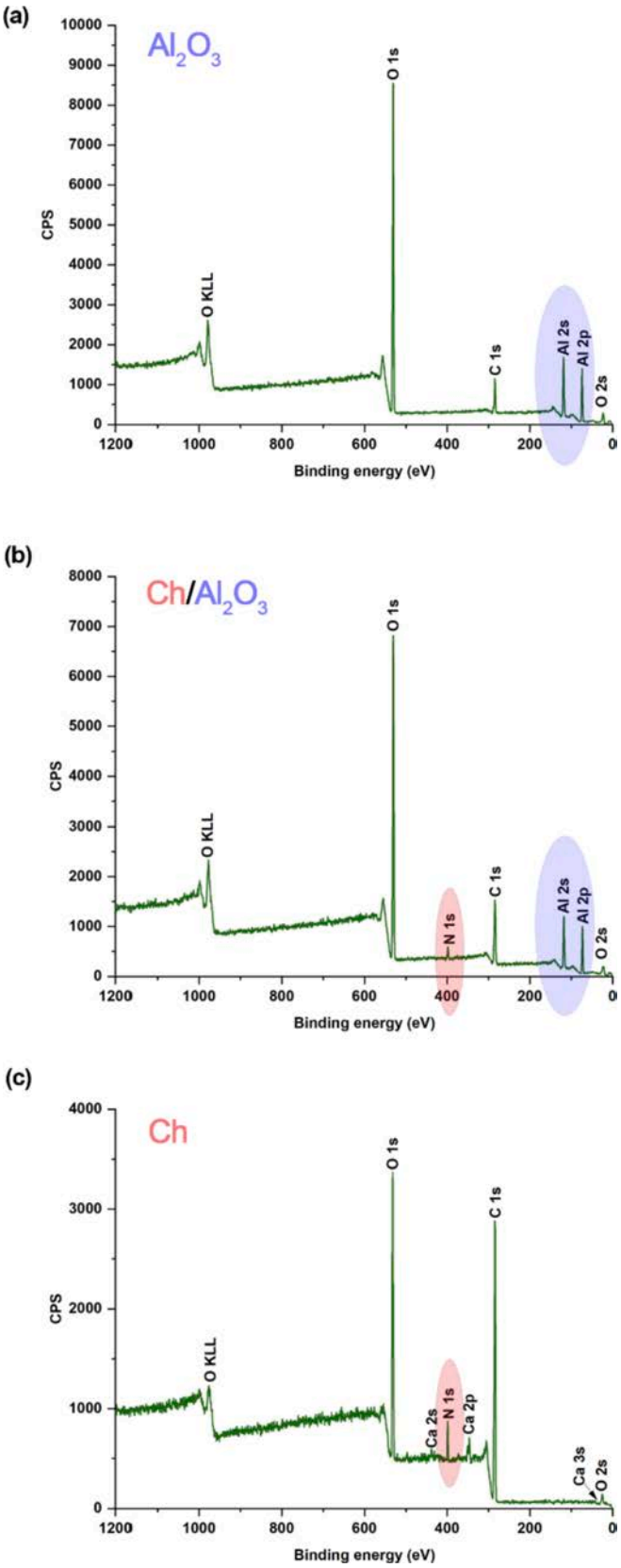

Fig. 9. The XPS spectra for: (a) Al_2O_3, (b) Ch/Al_2O_3 (middle) and (c) Ch.

surfactants in the samples and the low homogeneity of their distribution within the samples.

The high resolution XPS spectra of C 1s, O 1s, N 1s, and Al 2p (Figs. S6-S11) for all the studied multicomponent samples showed that the chemical bonds between the polymer and the adsorbent were formed. The assignation of the different chemical to the different peaks of the XPS spectra are reported in Table S1. In general, the content of carbon in the post-adsorption samples increased when compared to pre-adsorption ones (Table S2). In the composite materials, N and Al were detected, confirming adsorption. In such cases it is impossible to determine the concentration of carbon and nitrogen quantitatively because of the adventitious carbon and heterogeneity of the samples. The deconvolution of N 1s spectra of the samples yielded different outcomes (Fig. 10a-d).

In the case of Ch/FS-91/Al_2O_3 and Ch/A-Si/Al_2O_3, only the C-NH_2 bond is visible, whereas in the case of the Ch/Al_2O_3 and Ch/SDS/Al_2O_3 systems, an additional bond is visible (C-NH-C(=O)-). The nature of chitosan, which is deacetylated chitin, requires the presence of the acetylamine group. These finding overlap with the fact that the highest adsorption occurred in the case of the Ch/SDS/Al_2O_3 and Ch/Al_2O_3 systems, lower for the Ch/FS-91/Al_2O_3, and the lowest in the Ch/A-Si/Al_2O_3 system. This should be confirmed in further studies. Nevertheless at this point it looks like the higher adsorption takes place in the systems where not only the amine, but also acetylamine groups are found.

A last aspect that is interesting to evaluate related to the interaction of additive with alumina dispersions is the role of this additives in the dispersion stability. Fig. 11 presents the influence of chitosan/anionic surfactant (SDS, A-Si and FS-91) mixtures and chitosan alone on the stability of the Al_2O_3 dispersions as was evaluated by the time evolution of the absorbance of the samples a 500 nm.

The quick drop of absorbance down to values close to zero of alumina suspensions suggests its fast destabilization, resulting in unstable alumina suspensions without the additives (drop of the absorbance from 0.3897 (0 h) to 0.0266 (15 h)). The presence of a high molecular compound, such as chitosan, enhances the stability as the higher absorbance values (Abs_{0h} = 0.4562) and the smooth decrease in the absorbance value (Abs_{15h} = 0.1528) with time is evidenced, which corresponds with previous studies [63]. This can be explained by the fact at pH = 7 the

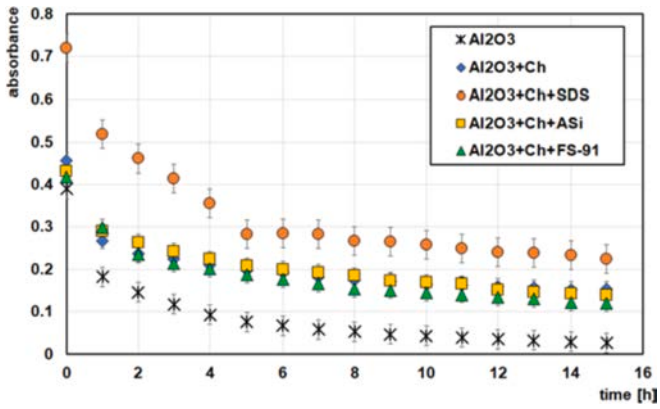

Fig. 11. Dependence of the absorbance at 500 nm on the time for alumina dispersions in presence of different additives. Chitosan concentration 400 ppm and surfactant concentrations (0.002 % v/v).

surface of alumina is slightly positively charged, and the adsorption of chitosan results from the hydrogen bonding and van der Waals interactions. The deprotonation of the amine groups of the chitosan chains indicates the formation of a collapse layer where chitosan chains adopt a coiled structures on the alumina surface. In such cases the increase in stability is the consequence of the (electro)steric stabilization. Therefore, the sixfold increase of stability measured in the 15 h when comparing Al_2O_3 and Ch/Al_2O_3 systems was observed. As the results show, the addition of the anionic surfactant can also help to improve stability. Stability is the highest for the SDS/Ch/Al_2O_3 system (Abs_{15h} = 0.2246), which is in line with the enhanced deposition of SDS/Ch complexes on the alumina surface in relation to the chitosan (see Fig. 7). The stability of the dispersions upon the adsorption of SDS/Ch complexes may be considered as being of electrosteric origin. The use of the other surfactant, A-Si and FS-91, also improves the stability of the Al_2O_3 suspensions, but the stability remains comparable to that obtained after the Ch addition (Ch/A-Si/Al_2O_3 Abs_{15h} = 0.1393; Ch/FS-91/Al_2O_3 Abs_{15h} = 0.1203). In these systems the most probable stability mechanism is a combination of electrosteric and depletion stabilization. This

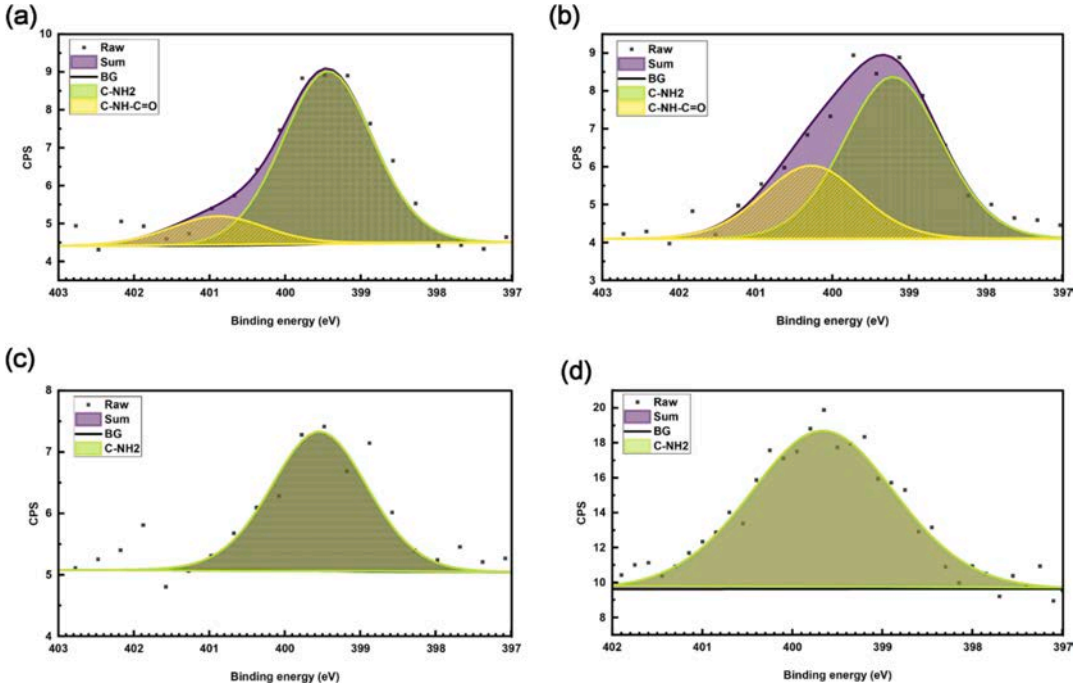

Fig. 10. N 1 s HRXPS spectra for (a) Ch/Al_2O_3, (b) Ch/SDS/Al_2O_3, (c) Ch/FS-91/Al_2O_3, (d) Ch/A-Si/Al_2O_3 samples.

means that a part of the formed Ch/A-100 and Ch/FS-91 complexes adsorbs on the alumina surface (electrosteric stabilization) whereas the rest remains in the bulk solution (depletion stabilization) [64,65].

5. Conclusions

This work has demonstrated that the addition of chitosan and chitosan/anionic surfactant mixtures to alumina dispersions can be exploited for providing an enhanced stability to alumina dispersion. This depends on the specific chemistry of the surfactant, which influences on their ability for the adsorption of the formed chitosan/anionic surfactant complexes on the alumina. The complexes can either adsorb on alumina surface, or remain in the bulk, providing different stabilization mechanisms. The highest adsorption and stability were obtained after the addition of SDS to the Ch/Al_2O_3 system, where the interactions between chitosan and SDS were found to be the strongest between all the studied mixtures. This resulted in the formation of complexes that can adsorb very efficiently on the alumina surface as was confirmed by the chitosan adsorption, elemental mapping and XPS measurements. Polymer-surfactant complexes are also formed in the case of the Ch/FS-91/Al_2O_3 and Ch/A-Si/Al_2O_3 systems. However, the adsorption affinity of those complexes toward the alumina surface is lower than for the Ch/SDS complexes, which results in weak adhesion of the complexes to the alumina surface (SEM-EDX mapping). The formed complexes most likely stay in the bulk of the suspension. Therefore, the observed stabilization is greater in the case of Ch/SDS/Al_2O_3 than in the Ch/FS-91/Al_2O_3 and Ch/A-Si/Al_2O_3 systems.

It can be also concluded that the addition of very small amounts of hydrocarbon surfactant (0.002 % v/v of SDS) can enhance the stability of the alumina suspensions. This means that the addition of common and relatively cheap surfactants decrease the economic impact (low price of the used reagent) associated with the stabilization of colloidal dispersion. The results have shown a fair increase in the stability of the colloidal system, which is a base for a great deal of industrial products. This opens very interesting perspectives for formulators to exploit the synergistic effect emerging from biopolymers occurring in conjunction with surfactants in the design of more efficient colloidal systems for industrial applications.

Declaration of Competing Interest

The authors declare that they have no known competing financial interests or personal relationships that could have appeared to influence the work reported in this paper.

Data availability

Data will be made available on request.

Acknowledgements

We would like to offer our gratitude to the employees of Analytical Laboratory: Aldona Nowicka, Ph.D., Anna Sobieszek, M.Sc., and Marcin Kuśmierz, Ph.D., for the SEM-EDX elemental mapping, and XPS measurements. The Authors would also like to acknowledge that the work was supported by subsidy from the Polish Ministry of Education and Science for the Faculty of Chemistry of Wroclaw University of Science and Technology as well as for the Institute of Chemical Sciences, Faculty of Chemistry, Maria Curie-Skłodowska University in Lublin. Eduardo Guzmán acknowledge the support by MICINN under Grant PID2019-106557GB-C21.

Appendix A. Supplementary data

Supplementary data to this article can be found online at https://doi.org/10.1016/j.cej.2022.138145.

References

[1] I. Hamed, F. Özogul, J.M. Regenstein, Industrial applications of crustacean by-products (chitin, chitosan, and chitooligosaccharides): A review, Trends Food Sci. Technol. 48 (2016) 40–50, https://doi.org/10.1016/J.TIFS.2015.11.007.
[2] I. Kardas, M.H. Struszczyk, M. Kucharska, L.A.M. van den Broek, J.E.G. van Dam, D. Ciechańska, Chitin and Chitosan as Functional Biopolymers for Industrial Applications, in: P. Navard (Ed.), The European Polysaccharide Network of Excellence (EPNOE), Springer Vienna, Vienna, 2013, pp. 329–373.
[3] G. Neeraj, S. Krishnan, P. Senthil Kumar, K.R. Shriaishvarya, V. Vinoth Kumar, Performance study on sequestration of copper ions from contaminated water using newly synthesized high effective chitosan coated magnetic nanoparticles, Journal of Molecular Liquids. 214 (2016) 335–346. 10.1016/J.MOLLIQ.2015.11.051.
[4] K. Esumi, N. Takei, T. Yoshimura, Antioxidant-potentiality of gold–chitosan nanocomposites, Colloids Surf., B 32 (2003) 117–123, https://doi.org/10.1016/S0927-7765(03)00151-6.
[5] M.N.V. Ravi Kumar, A review of chitin and chitosan applications, React. Funct. Polym. 46 (2000) 1–27, https://doi.org/10.1016/S1381-5148(00)00038-9.
[6] E.R. Welsh, C.L. Schauer, S.B. Qadri, R.R. Price, Chitosan Cross-Linking with a Water-Soluble, Blocked Diisocyanate. 1. Solid State, Biomacromolecules 3 (2002) 1370–1374, https://doi.org/10.1021/bm025625z.
[7] M. Kong, X.G. Chen, K. Xing, H.J. Park, Antimicrobial properties of chitosan and mode of action: A state of the art review, Int. J. Food Microbiol. 144 (2010) 51–63, https://doi.org/10.1016/J.IJFOODMICRO.2010.09.012.
[8] A.J. Varma, S.V. Deshpande, J.F. Kennedy, Metal complexation by chitosan and its derivatives: a review, Carbohydr. Polym. 55 (1) (2004) 77–93.
[9] S. Zhang, X. Liu, X. Jin, H. Li, J. Sun, X. Gu, The novel application of chitosan: Effects of cross-linked chitosan on the fire performance of thermoplastic polyurethane, Carbohydr. Polym. 189 (2018) 313–321, https://doi.org/10.1016/J.CARBPOL.2018.02.034.
[10] M. Hernández-Rivas, E. Guzmán, L. Fernández-Peña, A. Akanno, A. Greaves, F. Léonforte, F. Ortega, R.G. Rubio, G.S. Luengo, Deposition of Synthetic and Bio-Based Polycations onto Negatively Charged Solid Surfaces: Effect of the Polymer Cationicity, Ionic Strength, and the Addition of an Anionic Surfactant, Colloids and Interfaces. 4 (2020) 33, https://doi.org/10.3390/colloids4030033.
[11] T. Masilompane, N. Chaukura, A.K. Mishra, S.B. Mishra, B.B. Mamba, Lignin and Chitosan-Based Materials for Dye and Metal Ion Remediation in Aqueous Systems, (2018) 55–73. 10.1007/978-3-319-68708-7_3.
[12] R. Xiong, A.M. Grant, R. Ma, S. Zhang, V. v. Tsukruk,, Naturally-derived biopolymer nanocomposites: Interfacial design, properties and emerging applications, Materials Science and Engineering: R: Reports. 125 (2018) 1–41, https://doi.org/10.1016/J.MSER.2018.01.002.
[13] J. Matusiak, E. Grządka, A. Bastrzyk, Stability, adsorption and electrokinetic properties of the chitosan/silica system, Colloids Surf., A 554 (2018) 245–252, https://doi.org/10.1016/j.colsurfa.2018.06.056.
[14] R. Yang, H. Li, M. Huang, H. Yang, A. Li, A review on chitosan-based flocculants and their applications in water treatment, Water Res. 95 (2016) 59–89, https://doi.org/10.1016/J.WATRES.2016.02.068.
[15] D. Langevin, Complexation of oppositely charged polyelectrolytes and surfactants in aqueous solutions, A review, Advances in Colloid and Interface Science. 147–148 (2008) 170–177, https://doi.org/10.1016/j.cis.2008.08.013.
[16] S. Llamas, E. Guzmán, F. Ortega, N. Baghdadli, C. Cazeneuve, R.G. Rubio, G. S. Luengo, Adsorption of polyelectrolytes and polyelectrolytes-surfactant mixtures at surfaces: a physico-chemical approach to a cosmetic challenge, Adv. Colloid Interface Sci. 222 (2015) 461–487, https://doi.org/10.1016/j.cis.2014.05.007.
[17] T.D.A. Senra, S.P. Campana-Filho, J. Desbrières, Surfactant-polysaccharide complexes based on quaternized chitosan, Characterization and application to emulsion stability, European Polymer Journal. 104 (2018) 128–135, https://doi.org/10.1016/J.EURPOLYMJ.2018.05.002.
[18] L. Fernández-Peña, E. Guzmán, C. Fernández-Pérez, I. Barba-Nieto, F. Ortega, F. Leonforte, R.G. Rubio, G.S. Luengo, Study of the Dilution-Induced Deposition of Concentrated Mixtures of Polyelectrolytes and Surfactants, Polymers (Basel). 14 (2022) 1335, https://doi.org/10.3390/polym14071335.
[19] E. Guzmán, S. Llamas, A. Maestro, L. Fernández-Peña, A. Akanno, R. Miller, F. Ortega, R.G. Rubio, Polymer–surfactant systems in bulk and at fluid interfaces, Adv. Colloid Interface Sci. 233 (2016) 38–64, https://doi.org/10.1016/j.cis.2015.11.001.
[20] A. Fan, P. Somasundaran, N.J. Turro, Role of sequential adsorption of polymer/surfactant mixtures and their conformation in dispersion/flocculation of alumina, Colloids Surf., A 146 (1999) 397–403, https://doi.org/10.1016/S0927-7757(98)00865-6.
[21] A. Şakar-Deliormanlı, Synergistic effect of polymer-surfactant mixtures on the stability of aqueous silica suspensions, J Eur Ceram Soc. 27 (2007) 611–618, https://doi.org/10.1016/j.jeurceramsoc.2006.04.117.
[22] N. Khan, B. Brettmann, Intermolecular Interactions in Polyelectrolyte and Surfactant Complexes in Solution, Polymers (Basel). 11 (2018) 51, https://doi.org/10.3390/polym11010051.
[23] E. Grządka, J. Matusiak, A. Bastrzyk, I. Polowczyk, CMC as a stabiliser of metal oxide suspensions, Cellulose (2019), https://doi.org/10.1007/s10570-019-02930-y.
[24] A. Akanno, E. Guzmán, F. Ortega, R.G. Rubio, Behavior of the water/vapor interface of chitosan solutions with an anionic surfactant: effect of polymer–surfactant interactions, PCCP 22 (2020) 23360–23373, https://doi.org/10.1039/D0CP02470H.
[25] L. Fernández-Peña, I. Abelenda-Nuñez, M. Hernández-Rivas, F. Ortega, R.G. Rubio, E. Guzmán, Impact of the bulk aggregation on the adsorption of oppositely charged

polyelectrolyte-surfactant mixtures onto solid surfaces, Adv. Colloid Interface Sci. 282 (2020), 102203, https://doi.org/10.1016/j.cis.2020.102203.
[26] L.C. Becker, I. Boyer, W.F. Bergfeld, D.V. Belsito, R.A. Hill, C.D. Klaassen, D. C. Liebler, J.G. Marks, R.C. Shank, T.J. Slaga, P.W. Snyder, F.A. Andersen, L.J. Gill, Safety Assessment of Alumina and Aluminum Hydroxide as Used in Cosmetics, International Journal of Toxicology. 35 (2016) 16S–33S, https://doi.org/10.1177/1091581816677948.
[27] P. Hassanpour, Y. Panahi, A. Ebrahimi-Kalan, A. Akbarzadeh, S. Davaran, A. N. Nasibova, R. Khalilov, T. Kavetskyy, Biomedical applications of aluminium oxide nanoparticles, Micro & Nano Letters. 13 (2018) 1227–1231, https://doi.org/10.1049/MNL.2018.5070.
[28] N.M. Kovalchuk, A. Trybala, V. Starov, O. Matar, N. Ivanova, Fluoro- vs hydrocarbon surfactants: Why do they differ in wetting performance? Adv. Colloid Interface Sci. 210 (2014) 65–71, https://doi.org/10.1016/J.CIS.2014.04.003.
[29] J. O'Lenick, Silicone emulsions and surfactants, Journal of Surfactants and Detergents 2000 3:3. 3 (2000) 387–393. 10.1007/S11743-000-0143-Y.
[30] M.M. Singer, R.S. Tjeerdema, Fate and effects of the surfactant sodium dodecyl sulfate, Rev. Environ. Contam. Toxicol. 133 (1993) 95–149, https://doi.org/10.1007/978-1-4613-9529-4_3.
[31] J. Matusiak, E. Grządka, M. Paszkiewicz, J. Patkowski, Complexes of fluorinated, silicone and hydrocarbon surfactants with carboxymethylcellulose and their influence on properties of the alumina suspension, Colloid and Polymer, Science 297 (2019) 677–687, https://doi.org/10.1007/s00396-019-04494-6.
[32] S. Prochazkova, K.M. Vårum, K. Ostgaard, Quantitative determination of chitosans by ninhydrin, Carbohydr. Polym. 38 (1999) 115–122, https://doi.org/10.1016/S0144-8617(98)00108-8.
[33] E. Guzmán, L. Fernández-Peña, F. Ortega, R.G. Rubio, Equilibrium and kinetically trapped aggregates in polyelectrolyte–oppositely charged surfactant mixtures, Curr. Opin. Colloid Interface Sci. 48 (2020) 91–108, https://doi.org/10.1016/j.cocis.2020.04.002.
[34] E. Grządka, J. Matusiak, E. Godek, U. Maciołek, Mixtures of cationic guar gum and anionic surfactants as stabilizers of zirconia suspensions, J. Mol. Liq. 343 (2021), 117677, https://doi.org/10.1016/J.MOLLIQ.2021.117677.
[35] C.G. Bell, C.J.W. Breward, P.D. Howell, J. Penfold, R.K. Thomas, A theoretical analysis of the surface tension profiles of strongly interacting polymer–surfactant systems, J. Colloid Interface Sci. 350 (2010) 486–493, https://doi.org/10.1016/J.JCIS.2010.07.020.
[36] I. Varga, R.A. Campbell, General Physical Description of the Behavior of Oppositely Charged Polyelectrolyte/Surfactant Mixtures at the Air/Water Interface, Langmuir 33 (2017) 5915–5924, https://doi.org/10.1021/acs.langmuir.7b01288.
[37] A. Akanno, E. Guzmán, L. Fernández-Peña, F. Ortega, R.G. Rubio, Surfactant-Like Behavior for the Adsorption of Mixtures of a Polycation and Two Different Zwitterionic Surfactants at the Water/Vapor Interface, Molecules 24 (2019) 3442, https://doi.org/10.3390/molecules24193442.
[38] S.H. Lim, S.M. Hudson, Synthesis and antimicrobial activity of a water-soluble chitosan derivative with a fiber-reactive group, Carbohydr. Res. 339 (2004) 313–319, https://doi.org/10.1016/J.CARRES.2003.10.024.
[39] A.B. Vino, P. Ramasamy, V. Shanmugam, A. Shanmugam, Extraction, characterization and in vitro antioxidative potential of chitosan and sulfated chitosan from Cuttlebone of Sepia aculeata Orbigny, 1848, Asian Pacific Journal of Tropical Biomedicine. 2 (2012) S334–S341, https://doi.org/10.1016/S2221-1691(12)60184-1.
[40] C. Song, H. Yu, M. Zhang, Y. Yang, G. Zhang, Physicochemical properties and antioxidant activity of chitosan from the blowfly Chrysomya megacephala larvae, Int. J. Biol. Macromol. 60 (2013) 347–354, https://doi.org/10.1016/J.IJBIOMAC.2013.05.039.
[41] M.F. Queiroz, K.R.T. Melo, D.A. Sabry, G.L. Sassaki, H.A.O. Rocha, Does the Use of Chitosan Contribute to Oxalate Kidney Stone Formation?, Marine Drugs 2015, Vol. 13, Pages 141-158. 13 (2014) 141–158. 10.3390/MD13010141.
[42] H. Moussout, M. Aazza, H. Ahlafi, Thermal degradation characteristics of chitin, chitosan, Al2O3/chitosan, and benonite/chitosan nanocomposites, Handbook of Chitin and Chitosan: Volume 2: Composites and Nanocomposites from Chitin and Chitosan, Manufacturing and Characterisations. (2020) 139–174, https://doi.org/10.1016/B978-0-12-817968-0.00005-6.
[43] H. Moussout, H. Ahlafi, M. Aazza, A. Amechrouq, Al2O3/chitosan nanocomposite: Preparation, characterization and kinetic study of its thermal degradation, Thermochim Acta 668 (2018) 169–177, https://doi.org/10.1016/J.TCA.2018.08.023.
[44] K. Atrak, A. Ramazani, S. Taghavi Fardood, Green synthesis of amorphous and gamma aluminum oxide nanoparticles by tragacanth gel and comparison of their photocatalytic activity for the degradation of organic dyes, J. Mater. Sci.: Mater. Electron. 29 (2018) 8347–8353, https://doi.org/10.1007/S10854-018-8845-2.
[45] C. Liu, K. Shih, Y. Gao, F. Li, L. Wei, Dechlorinating transformation of propachlor through nucleophilic substitution by dithionite on the surface of alumina, J. Soils Sediments 12 (2012) 724–733, https://doi.org/10.1007/S11368-012-0506-0.
[46] I. Rutkowska, J. Marchewka, P. Jeleń, M. Odziomek, M. Korpyś, J. Paczkowska, M. Sitarz, Chemical and Structural Characterization of Amorphous and Crystalline Alumina Obtained by Alternative Sol–Gel Preparation Routes, Materials 2021, Vol. 14, Page 1761. 14 (2021) 1761. 10.3390/MA14071761.
[47] A.A. Tsyganenko, P.P. Mardilovich, Structure of alumina surfaces, J. Chem. Soc., Faraday Trans. 92 (1996) 4843, https://doi.org/10.1039/ft9969204843.
[48] T.D. Pham, M. Kobayashi, Y. Adachi, Adsorption of anionic surfactant sodium dodecyl sulfate onto alpha alumina with small surface area, Colloid and Polymer, Science 293 (2015) 217–227, https://doi.org/10.1007/S00396-014-3409-3.
[49] T.M.T. Nguyen, T.P.T. Do, T.S. Hoang, N.V. Nguyen, H.D. Pham, T.D. Nguyen, T.N. M. Pham, T.S. Le, T.D. Pham, Adsorption of anionic surfactants onto alumina: Characteristics, mechanisms, and application for heavy metal removal, International Journal of Polymer Science. 2018 (2018), https://doi.org/10.1155/2018/2830286.
[50] K. Esumi, H. Otsuka, K. Meguro, Adsorption of binary mixtures of hydrocarbon and fluorocarbon surfactants on alumina, J. Colloid Interface Sci. 142 (1991) 582–588, https://doi.org/10.1016/0021-9797(91)90088-P.
[51] F. Shahidi, J.K.V. Arachchi, Y.J. Jeon, Food applications of chitin and chitosans, Trends Food Sci. Technol. 10 (1999) 37–51, https://doi.org/10.1016/S0924-2244(99)00017-5.
[52] P.M. Claesson, B.W. Ninham, pH-dependent interactions between adsorbed chitosan layers, Langmuir 8 (2002) 1406–1412, https://doi.org/10.1021/LA00041A027.
[53] S.P. Strand, T. Tømmeraas, K.M. Vårum, K. Østgaard, Electrophoretic light scattering studies of chitosans with different degrees of N-acetylation, Biomacromolecules 2 (2001) 1310–1314, https://doi.org/10.1021/BM015598X.
[54] H. Liu, C. Wang, S. Zou, Z. Wei, Z. Tong, Simple, reversible emulsion system switched by pH on the basis of chitosan without any hydrophobic modification, Langmuir 28 (2012) 11017–11024, https://doi.org/10.1021/LA3021113.
[55] K.M. Vårum, M.H. Ottøy, O. Smidsrød, Water-solubility of partially N-acetylated chitosans as a function of pH: effect of chemical composition and depolymerisation, Carbohydr. Polym. 25 (1994) 65–70, https://doi.org/10.1016/0144-8617(94)90140-6.
[56] K.C.M. Kwok, L.F. Koong, G. Chen, G. McKay, Mechanism of arsenic removal using chitosan and nanochitosan, J. Colloid Interface Sci. 416 (2014) 1–10, https://doi.org/10.1016/J.JCIS.2013.10.031.
[57] G. Crini, Recent developments in polysaccharide-based materials used as adsorbents in wastewater treatment, Prog. Polym. Sci. 30 (2005) 38–70, https://doi.org/10.1016/J.PROGPOLYMSCI.2004.11.002.
[58] C.N. Costa, V.G. Teixeira, M.C. Delpech, J.V.S. Souza, M.A.S. Costa, Viscometric study of chitosan solutions in acetic acid/sodium acetate and acetic acid/sodium chloride, Carbohydr. Polym. 133 (2015) 245–250, https://doi.org/10.1016/J.CARBPOL.2015.06.094.
[59] E. Guzmán, L. Fernández-Peña, G.S. Luengo, A. Rubio, A. Rey, F. Léonforte, Self-Consistent Mean Field Calculations of Polyelectrolyte-Surfactant Mixtures in Solution and upon Adsorption onto Negatively Charged Surfaces, Polymers (Basel). 12 (2020) 624, https://doi.org/10.3390/polym12030624.
[60] E. Guzmán, S. Llamas, L. Fernández-Peña, F. Léonforte, N. Baghdadli, C. Cazeneuve, F. Ortega, R.G. Rubio, G.S. Luengo, Effect of a natural amphoteric surfactant in the bulk and adsorption behavior of polyelectrolyte-surfactant mixtures, Colloids Surf., A 585 (2020), 124178, https://doi.org/10.1016/j.colsurfa.2019.124178.
[61] J. Matusiak, E. Grządka, Cationic starch as the effective flocculant of silica in the presence of different surfactants, Sep. Purif. Technol. 234 (2020) 116132.
[62] L. Fernández-Peña, E. Guzmán, F. Leonforte, A. Serrano-Pueyo, K. Regulski, L. Tournier-Couturier, F. Ortega, R.G. Rubio, G.S. Luengo, Effect of molecular structure of eco-friendly glycolipid biosurfactants on the adsorption of hair-care conditioning polymers, Colloids Surf., B 185 (2020), 110578, https://doi.org/10.1016/j.colsurfb.2019.110578.
[63] E. Grządka, J. Matusiak, E. Godek, Alginic acid as a stabilizer of zirconia suspensions in the presence of cationic surfactants, Carbohydr. Polym. 246 (2020), 116634, https://doi.org/10.1016/j.carbpol.2020.116634.
[64] G. Fritz, V. Schädler, N. Willenbacher, N.J. Wagner, Electrosteric Stabilization of Colloidal Dispersions, Langmuir 18 (2002) 6381–6390, https://doi.org/10.1021/LA015734J.
[65] A.N. Semenov, A.A. Shvets, Theory of colloid depletion stabilization by unattached and adsorbed polymers, Soft Matter 11 (2015) 8863–8878, https://doi.org/10.1039/C5SM01365H.

SUPPLEMENTARY MATERIAL

The journey of tuning chitosan properties in colloidal systems: interactions with surfactants in the bulk and on the alumina surface

J. Matusiak[1*], E. Grządka[2], U. Maciołek[3], E. Godek[2], E. Guzmán[4,5]

1) Faculty of Chemistry, Wroclaw University of Science and Technology, Wybrzeże Wyspiańskiego 27, 50-370 Wroclaw, Poland
2) Department of Physical Chemistry, Institute of Chemical Sciences, Faculty of Chemistry, Maria Curie-Sklodowska University in Lublin, M. Curie-Sklodowska Sq. 3, Lublin, 20-031, Poland
3) Analytical Laboratory, Institute of Chemical Sciences, Faculty of Chemistry, Maria Curie-Sklodowska University in Lublin, M. Curie-Sklodowska Sq. 3, Lublin, 20-031, Poland
4) Departamento de Química Física, Facultad de Ciencias Químicas, Universidad Complutense de Madrid, Ciudad Universitaria s/n, 28040 Madrid, Spain
5) Unidad de Materia Condensada, Instituto Pluridisciplinar, Universidad Complutense de Madrid, Paseo Juan XXIII 1, 28040 Madrid, Spain

[*] Corresponding author e-mail: jakub.matusiak@pwr.edu.pl

TEM – Sample preparation

The alumina samples were dried and ground to fine powders in an agate mortar. Then the obtained powder was poured with 99.8% ethanol (POCH) to form a slurry that was subsequently inserted into an ultrasonic homogenizer for 10 s (Omni Sonic Ruptor 400, Omni International, Kenessaw, GE, USA). The slurry was pipetted and supported on a 300 mesh copper grid covered with the lacey formvar and stabilized with carbon (Ted Pella Company, Redding, CA, USA) and left on a filter paper for ethanol evaporation. The samples deposited on the grid were inserted into a single-tilt holder and moved to the electron microscope. The high-resolution electron microscope Titan G2 60–300 kV (FEI Company, Hilsboro, OR, USA) was used to display the studied materials. Microscopic studies were carried out at an accelerating voltage of the electron beam equal to 300 kV for the materials.

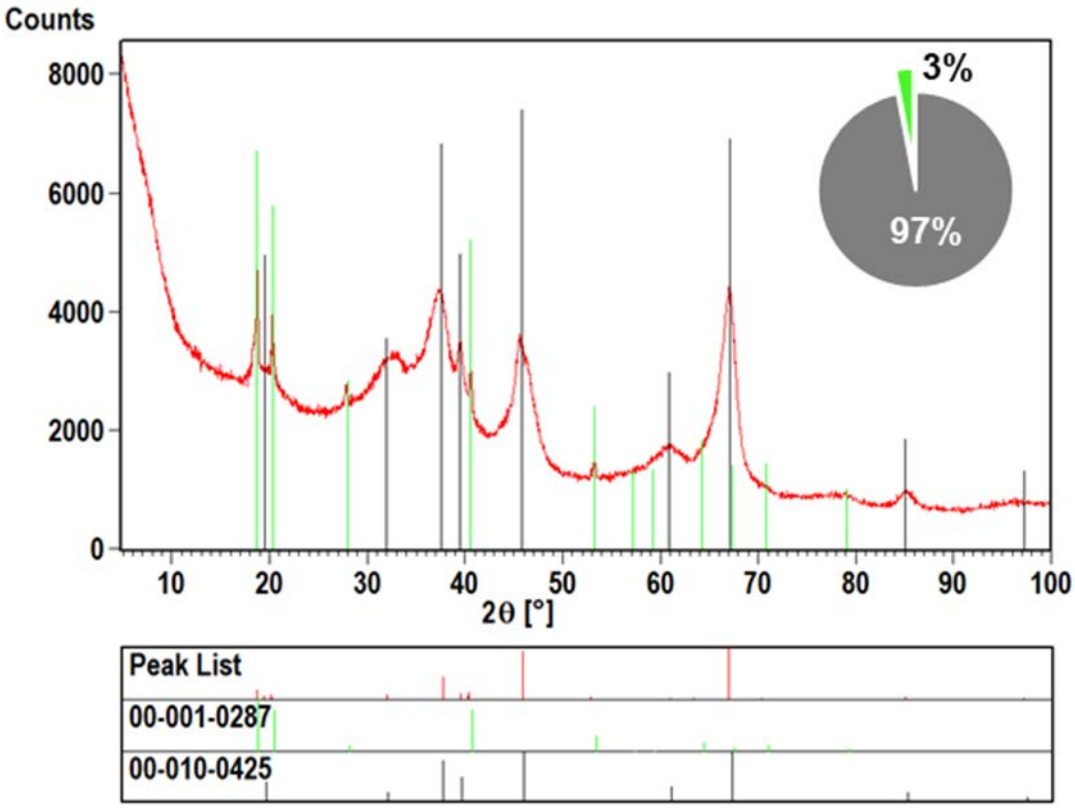

Fig. S1. Identification of crystalline phases of alumina. The presence of Al_2O_3 (Ref. Code 00-010-0425) and hydrated Al_2O_3 (Ref. Code 00-001-0287) was confirmed using the ICDD PDF4+2022 diffraction database.

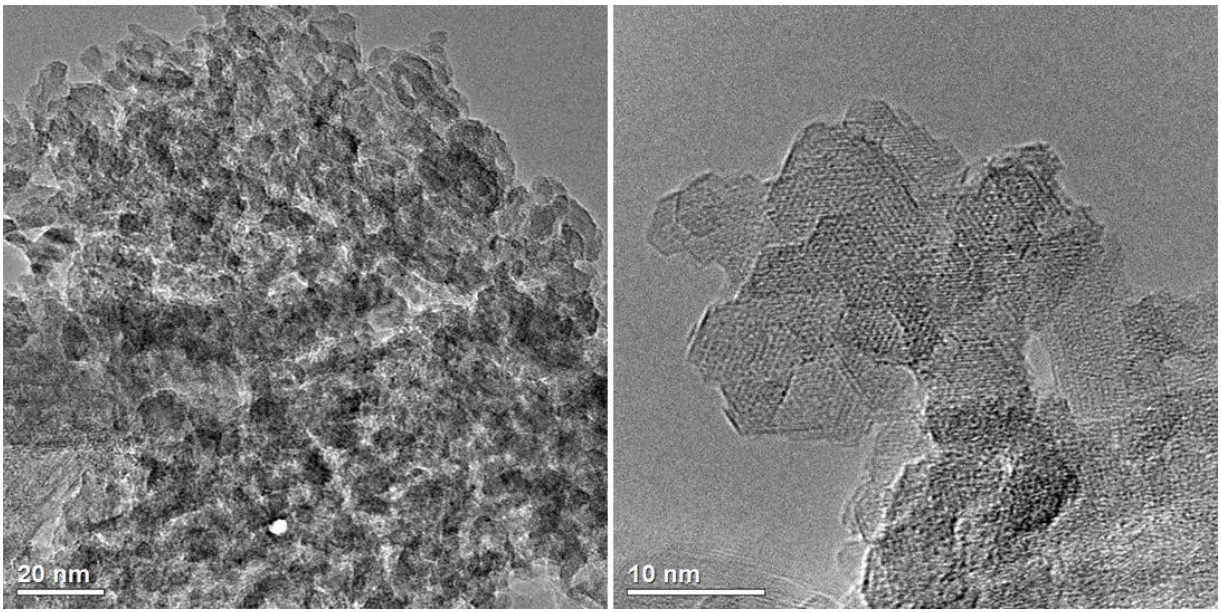

Fig. S2. TEM images of the used Al_2O_3.

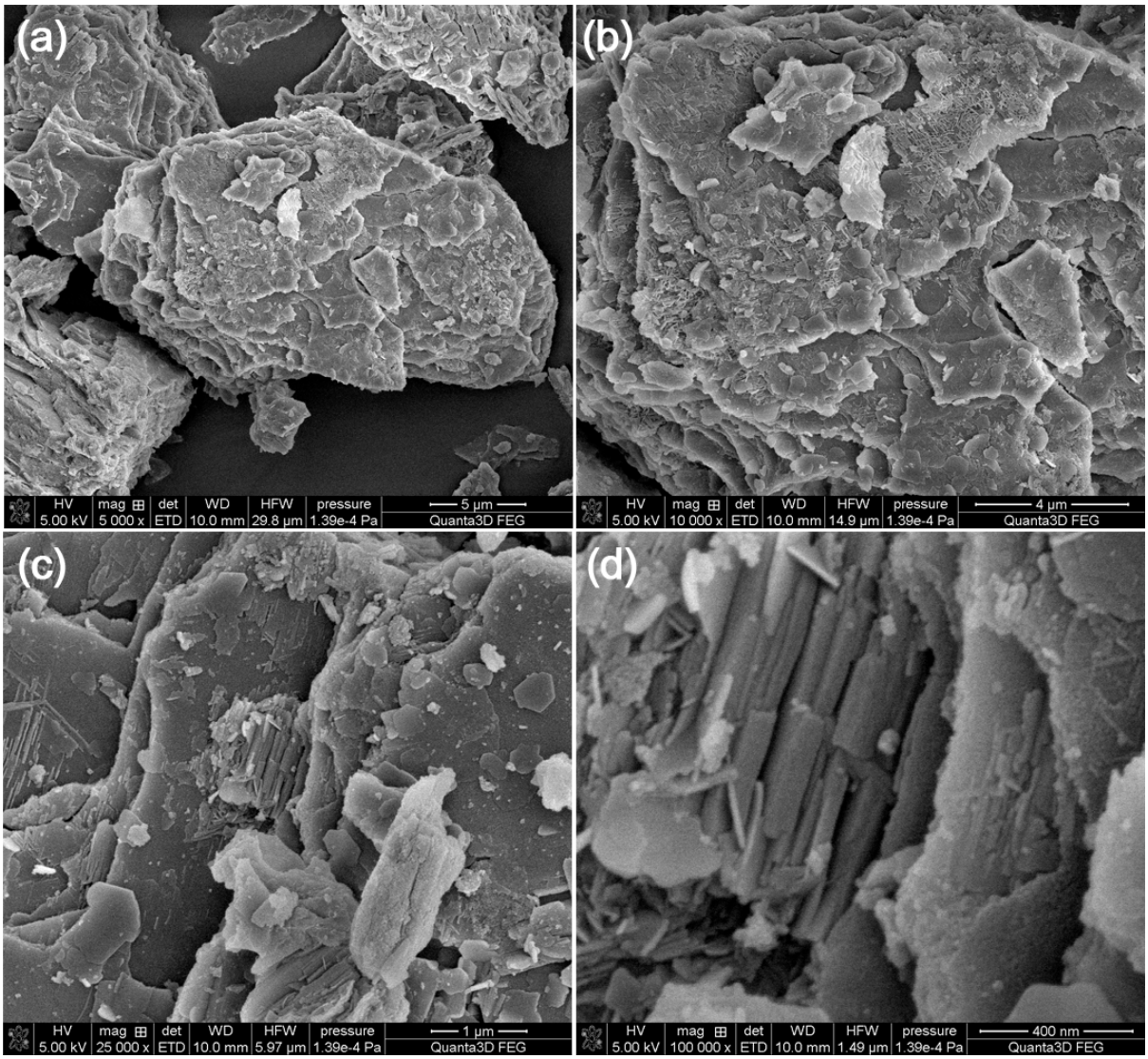

Fig. S3. High resolution SEM micrographs of the used Al_2O_3 with different magnification: (a) 5000x, (b) 10 000x, (c) 25 000x, (d) 100 000x.

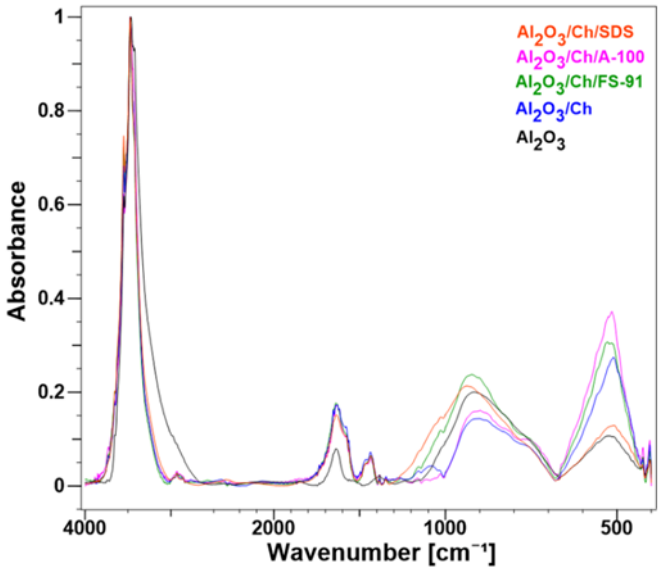

Fig. S4. Comparison of normalized FTIR spectra of unmodified alumina, Al_2O_3/Ch and Al_2O_3/Ch/surfactants systems.

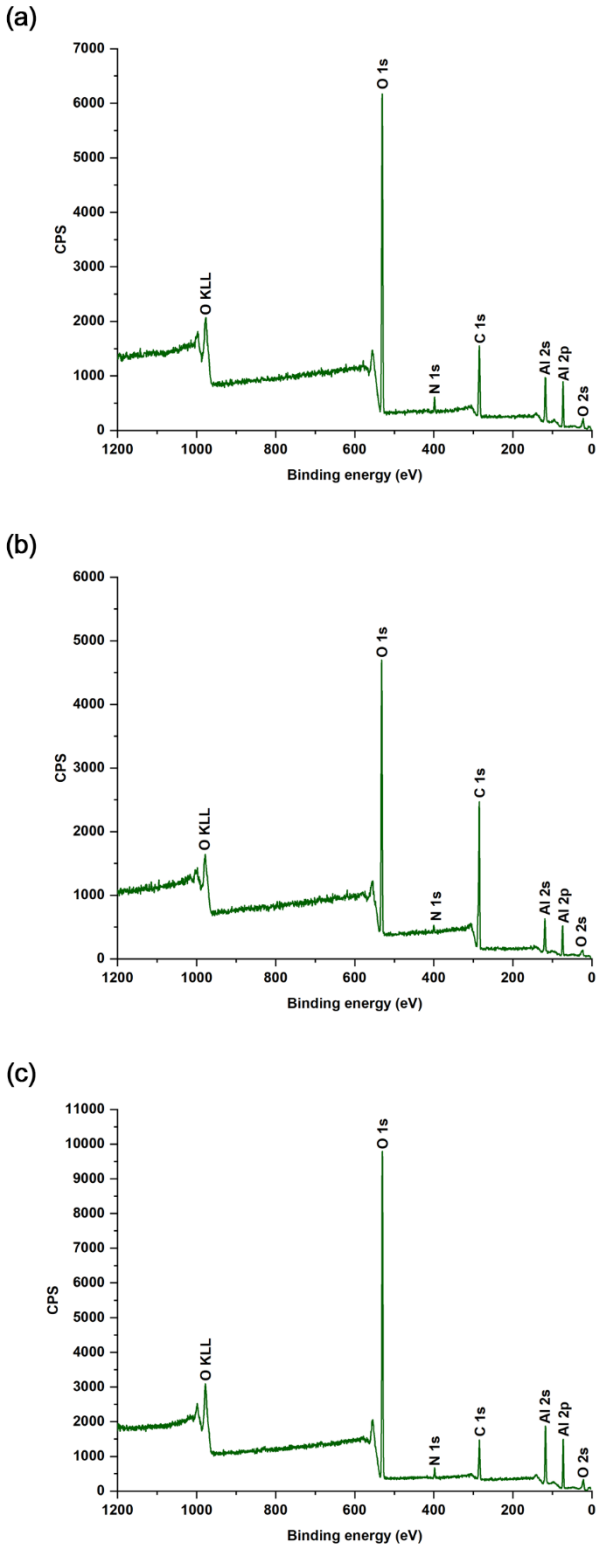

Fig. S5. The XPS survey spectra for: (a) Ch/SDS/Al_2O_3, (b) Ch/FS-91/Al_2O_3 and (c) Ch/A-Si/Al_2O_3 mixtures.

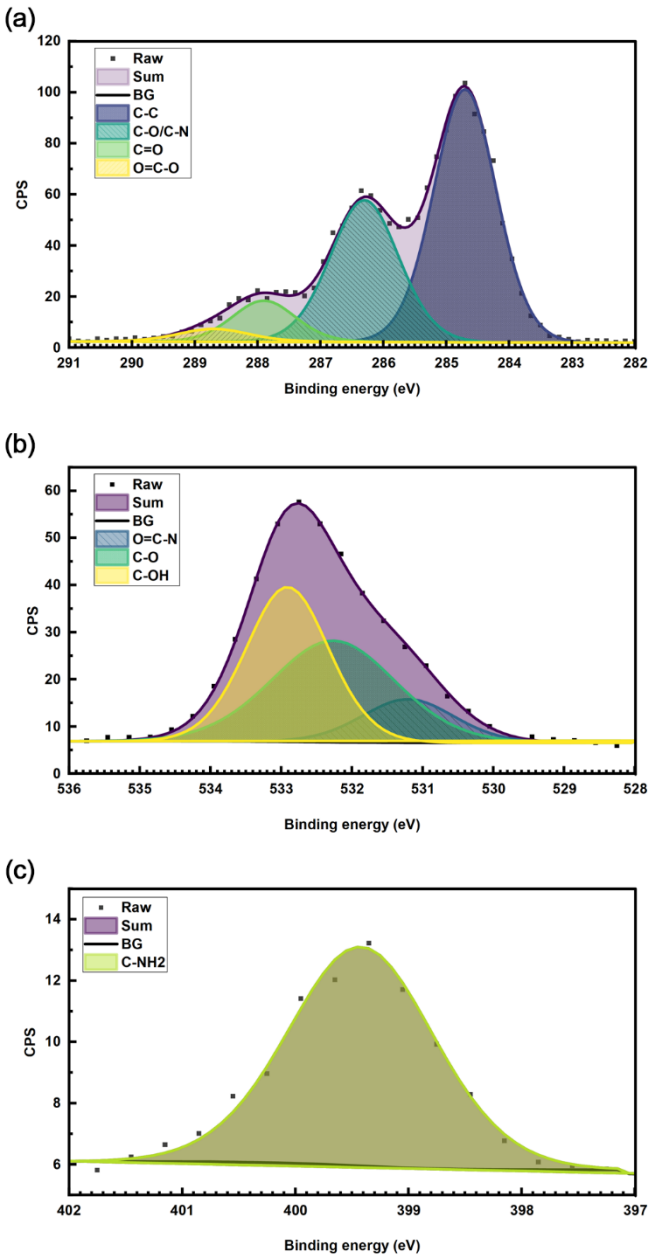

Fig. S6. HRXPS spectra of Ch sample: (a) C 1s, (b) O 1s, (c) N 1s.

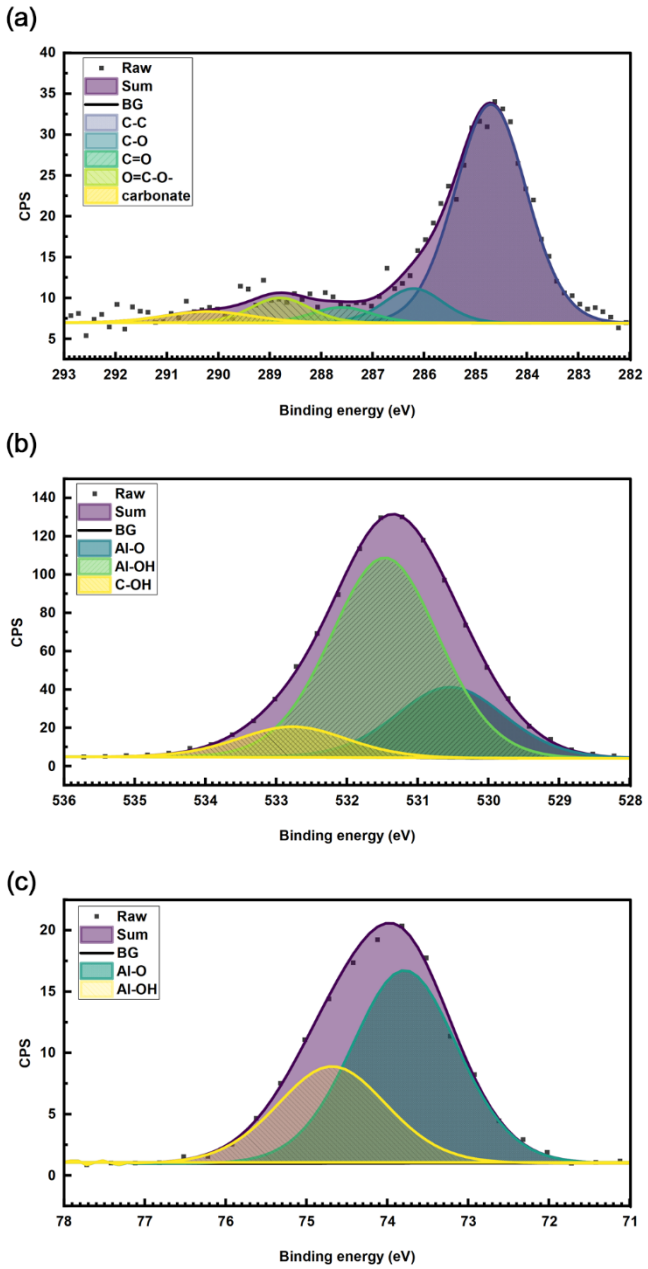

Fig. S7. HRXPS spectra of Al_2O_3 sample: (a) C 1s, (b) O 1s, (c) Al 2p.

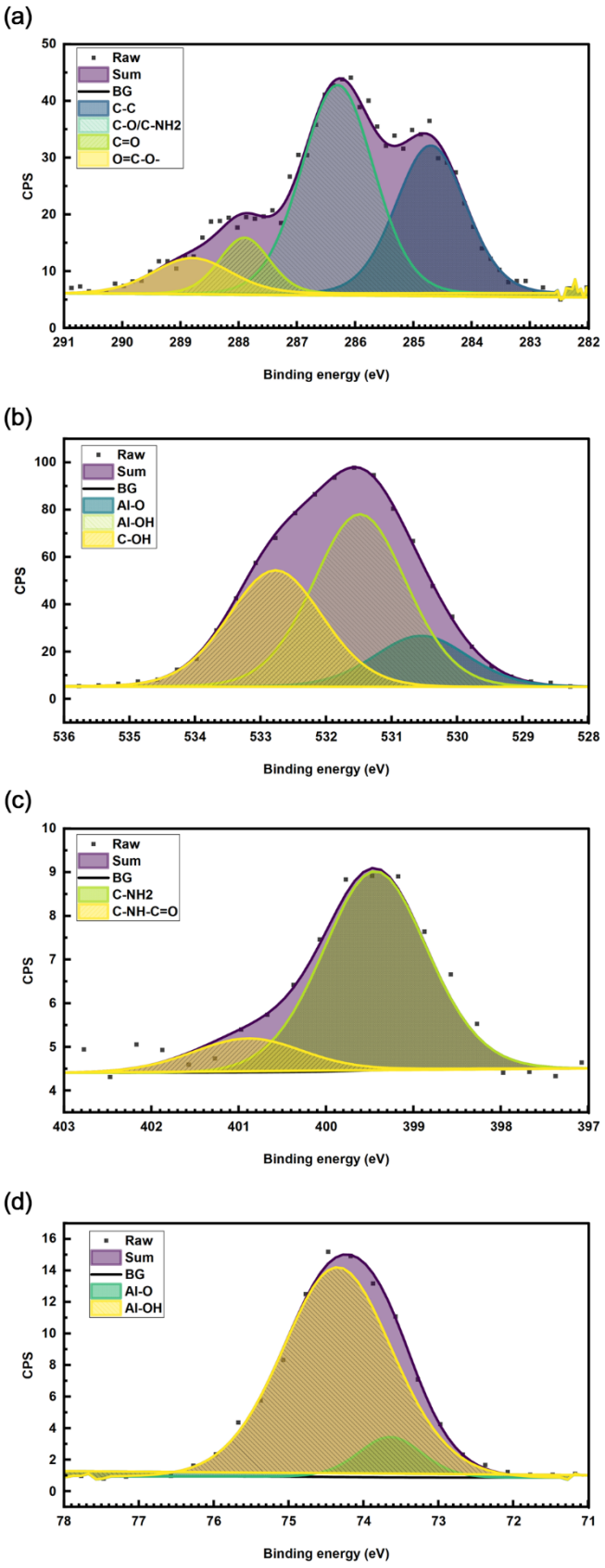

Fig. S8. HRXPS spectra of Ch/Al_2O_3 sample: (a) C 1s, (b) O 1s, (c) N 1s, (d) Al 2p.

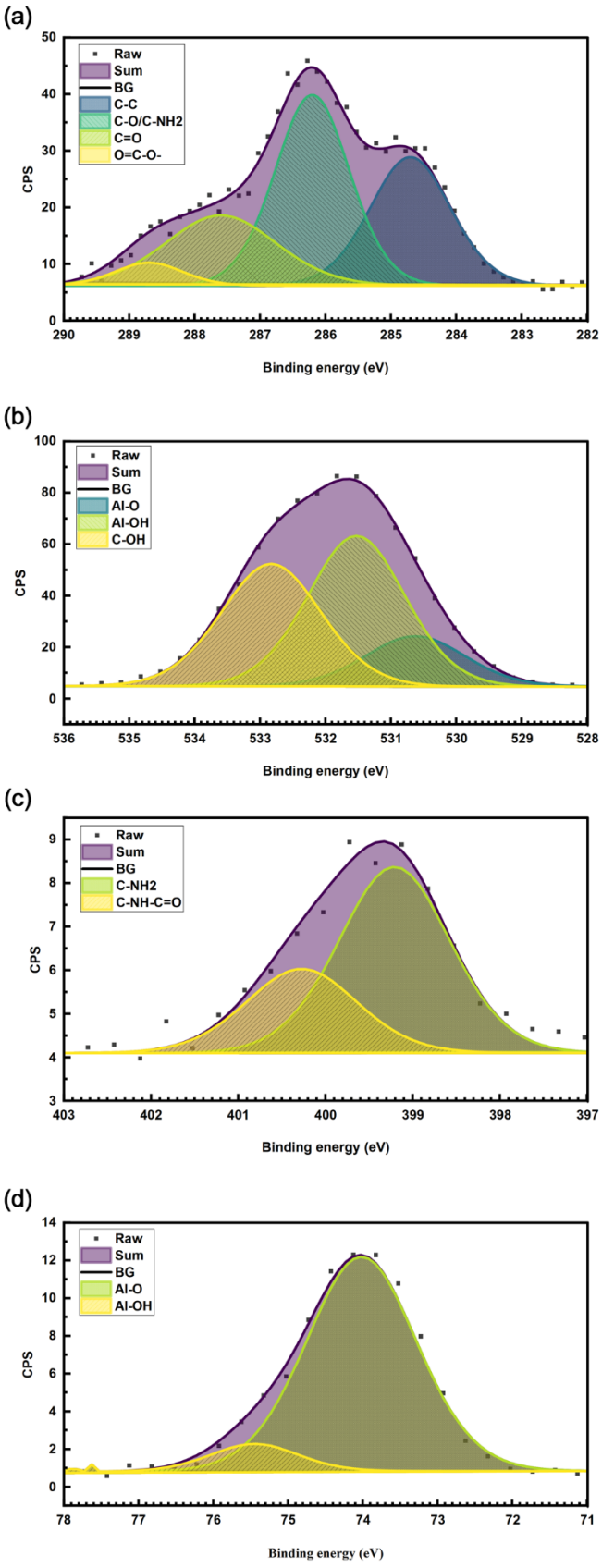

Fig. S9. HRXPS spectra of Ch/SDS/Al_2O_3 sample: (a) C 1s, (b) O 1s, (c) N 1s, (d) Al 2p.

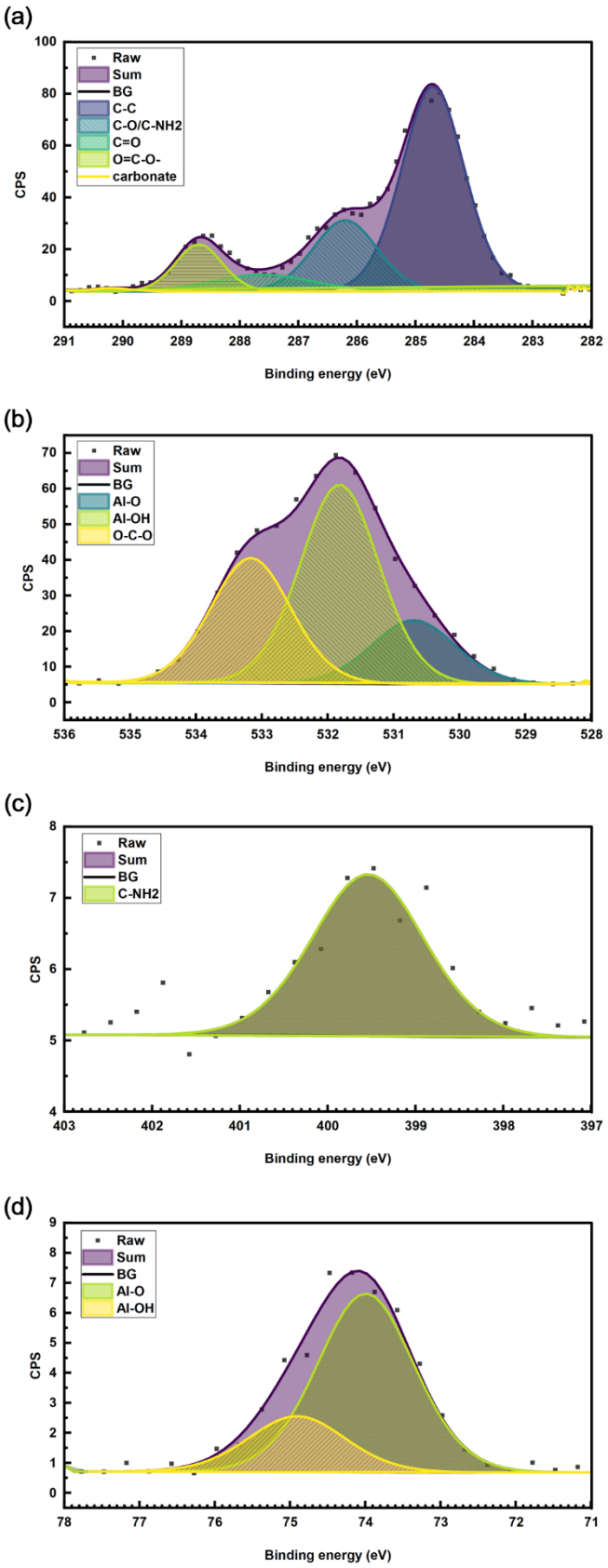

Fig. S10. HRXPS spectra of Ch/FS-91/Al_2O_3 sample: (a) C 1s, (b) O 1s, (c) N 1s, (d) Al 2p.

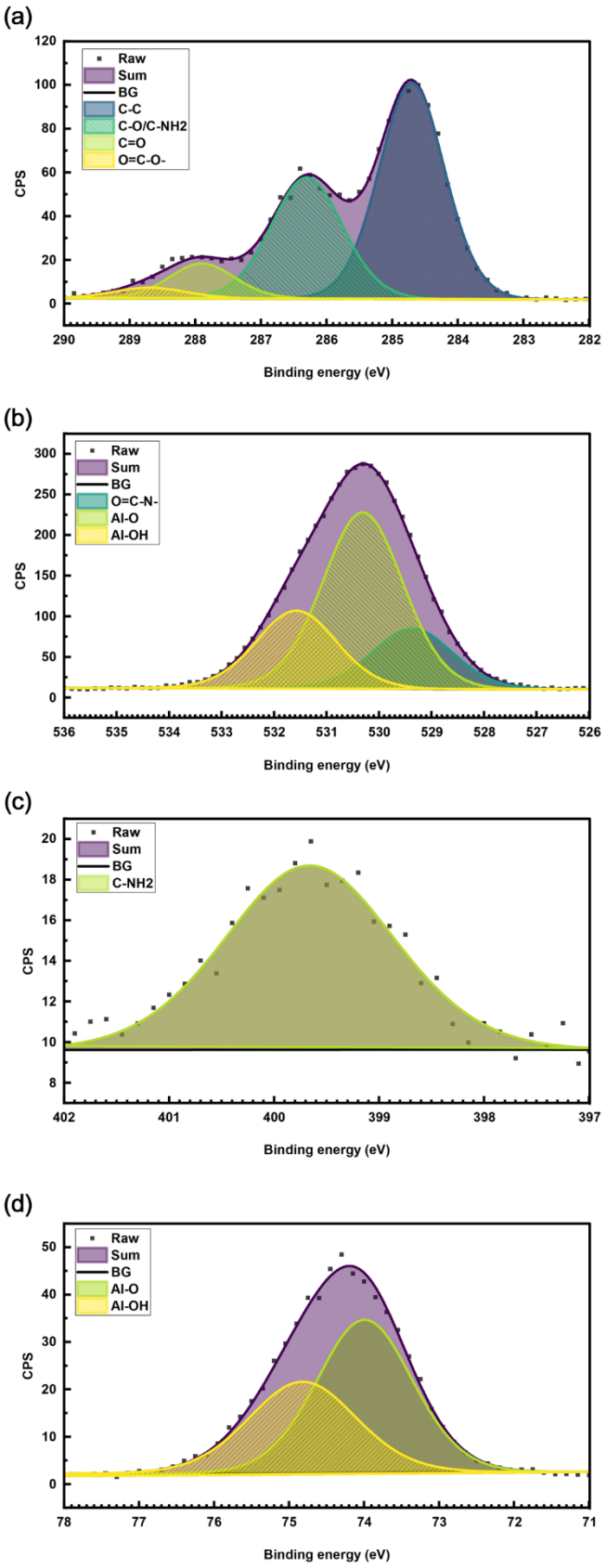

Fig. S11. HRXPS spectra of Ch/A-Si/Al_2O_3 sample: (a) C 1s, (b) O 1s, (c) N 1s, (d) Al 2p.

Table S1. Assignation of different peaks of the XPS spectra to specific chemical bonds.

Sample	Region	Name	Position [eV]	Origin
Ch	C 1s	C-C	284.7	Ch/Adv. C
		C-O	286.3	Ch/Adv. C
		C=O	287.9	Ch/Adv. C
		O=C-O-	288.7	Adv. C
	O 1s	O=C-N	531.21	Ch/Adv. C
		C-O	532.26	Ch/Adv. C
		C-OH aliphatic	532.91	Ch/Adv. C
	N 1s	C-NH_2	399.42	Ch
Al_2O_3	C 1s	C-C	284.7	Adv. C
		C-O	286.2	Adv. C
		C=O	287.6	Adv. C
		O=C-O-	288.8	Adv. C
		carbonate	290.2	Adv. C
	O 1s	Al-O	530.54	Al_2O_3
		Al-OH	531.46	Al_2O_3
		C-OH	532.77	Adv. C
	Al 2p	Al-O	73.79	Al_2O_3
		Al-OH	74.68	Al_2O_3
Ch/Al_2O_3	C 1s	C-C	284.7	Ch/Adv. C
		C-O, C-NH_2	286.3	Ch/Adv. C
		C=O	287.9	Ch/Adv. C
		O=C-O-	288.8	Adv. C
	O 1s	Al-O	530.54	Al_2O_3
		Al-OH	531.46	Al_2O_3
		C-OH	532.77	Adv. C
	N 1s	C-NH_2	399.44	Ch
		C-NH-C=O	400.89	Ch
Ch/SDS/Al_2O_3	C 1s	C 1s C-C	284.7	Ch/Adv. C
		C-O, C-NH_2	286.3	Ch/Adv. C
		C=O	287.9	Ch/Adv. C
		O=C-O-	288.8	Adv. C
	O 1s	Al-O	530.54	Al_2O_3
		Al-OH	531.46	Al_2O_3
		C-OH	532.77	Adv. C
	N 1s	C-NH_2	399.44	Ch
		C-NH-C=O	400.89	Ch
Ch/FS-91/Al_2O_3	C 1s	C-C	284.7	Ch/Adv. C
		C-O, C-NH_2	286.2	Ch/Adv. C
		C=O	287.6	Ch/Adv. C
		O=C-O-	288.7	Adv. C
		carbonate	290.2	Adv. C
	O 1s	Al-O	530.69	Al_2O_3
		Al-OH	531.82	Al_2O_3
		O-C-O	533.17	Ch/Adv. C

	N 1s	C-NH_2	399.54	Ch
Ch/A-Si/Al_2O_3	C 1s	C-C	284.7	Ch/Adv. C
		C-O, C-NH_2	286.3	Ch/Adv. C
		C=O	287.9	Ch/Adv. C
	O 1s	O=C-N-	529.36	Ch
		Al-O	530.31	Al_2O_3
		Al-OH	531.57	Al_2O_3
	N 1s	C-NH_2	399.66	Ch

Table S2. Elemental composition of the studied samples.

Sample	**Name**	**Position [eV]**	**%At. conc.**
Ch	C 1s	284.7	73.06
	O 1s	532.2	22.28
	Ca 2p	346.95	1.54
	N 1s	398.7	3.12
Al_2O_3	Al 2p	73.95	37.79
	C 1s	284.7	14.96
	O 1s	530.7	47.25
Ch/Al_2O_3	C 1s	284.7	29.22
	O 1s	530.7	41.81
	Al 2p	73.2	26.57
	N 1s	398.7	2.4
Ch/SDS/Al_2O_3	C 1s	284.7	30.95
	N 1s	397.95	2.44
	O 1s	530.7	41.55
	Al 2p	73.2	25.06
Ch/FS-91/Al_2O_3	C 1s	284.7	51.34
	O 1s	532.2	32.2
	Al 2p	73.95	15.36
	N 1s	400.2	1.1
Ch/A-Si/Al_2O_3	C 1s	284.7	17.86
	Al 2p	72.7	32.2
	O 1s	530.2	48.01
	N1s	398.2	1.93